UNIVERZITA KARLOVA

Avec le soutien de la Wallonie

fnrs LA LIBERTÉ DE CHERCHER

LIÈGE université Urban & Environmental Engineering

31st INTERNATIONAL CONFERENCE

PRAGUE GEOTECHNICAL DAYS 2025

ROCK MECHANICS IN ENGINEERING PRACTICE

Using numerical modelling for the design of Nuclear Waste Geological disposal

Frédéric COLLIN, Benoit PARDOEN, Gilles CORMAN, Hangbiao SONG

26-05-2025

A story of energy

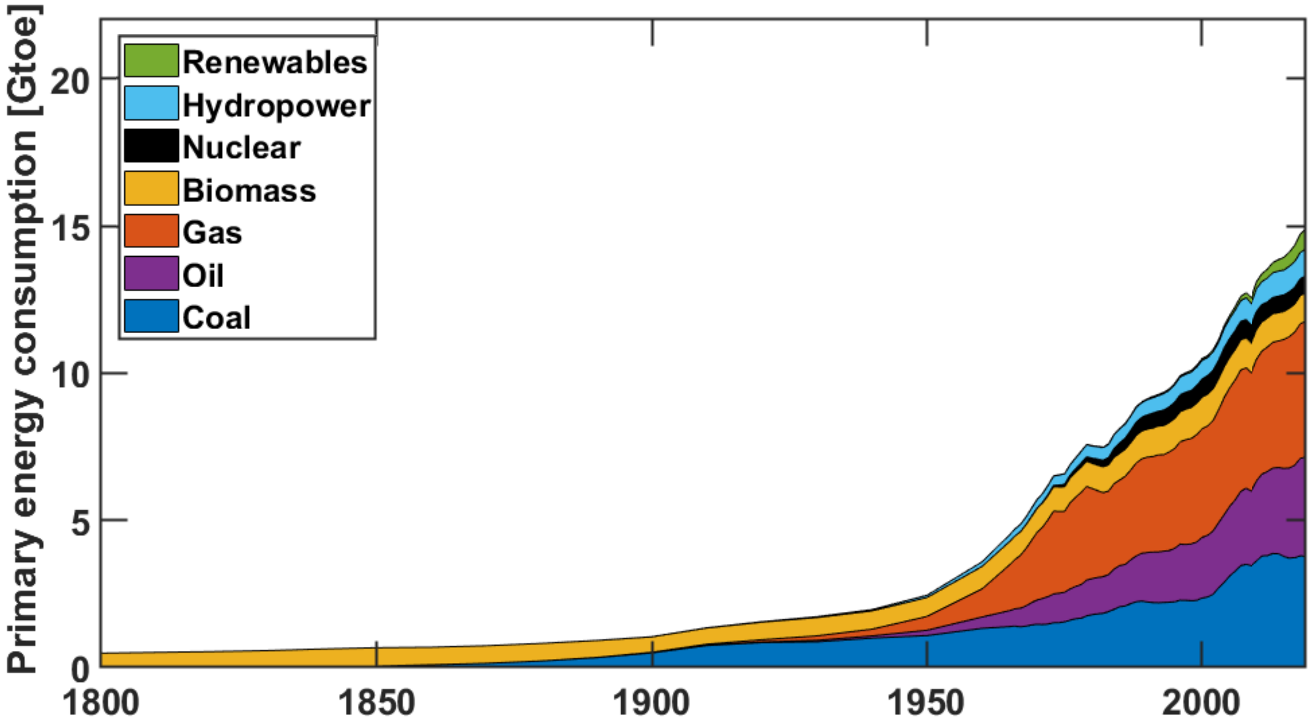

Data from [BP, 2022] & [Smil, 2016].

A story of energy

LIÈGE université
Urban & Environmental Engineering

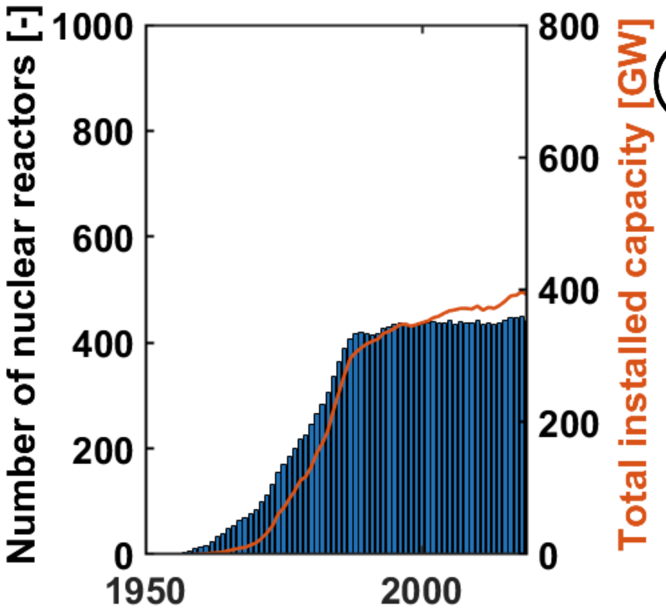

Data from [IAEA, 2021].

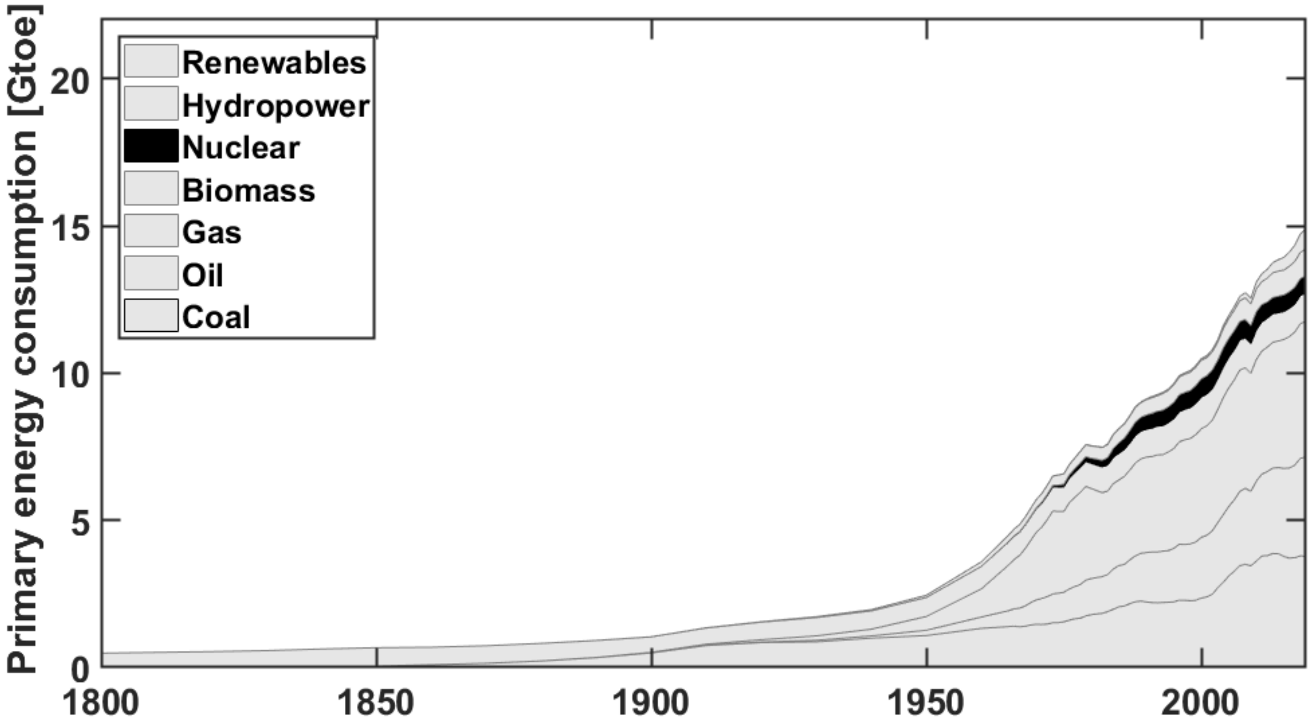

Data from [BP, 2022] & [Smil, 2016].

A story of energy

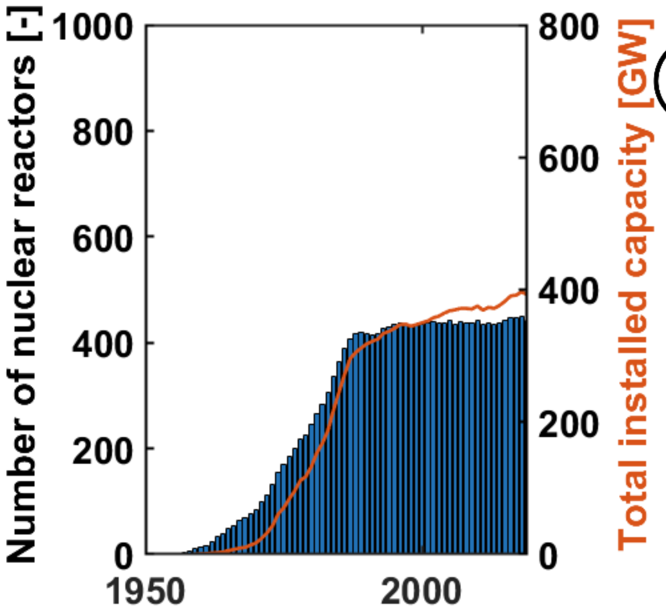

Data from [IAEA, 2021].

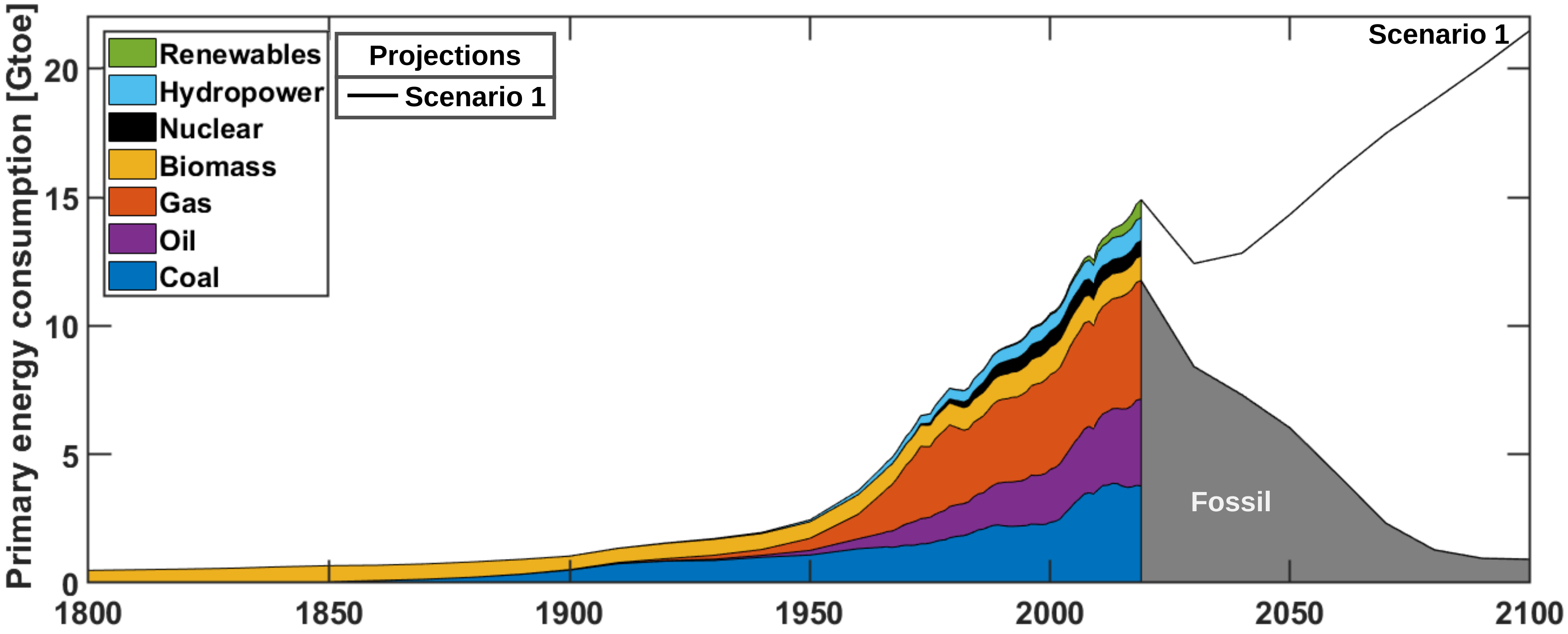

Data from [BP, 2022] & [Smil, 2016].

A story of energy

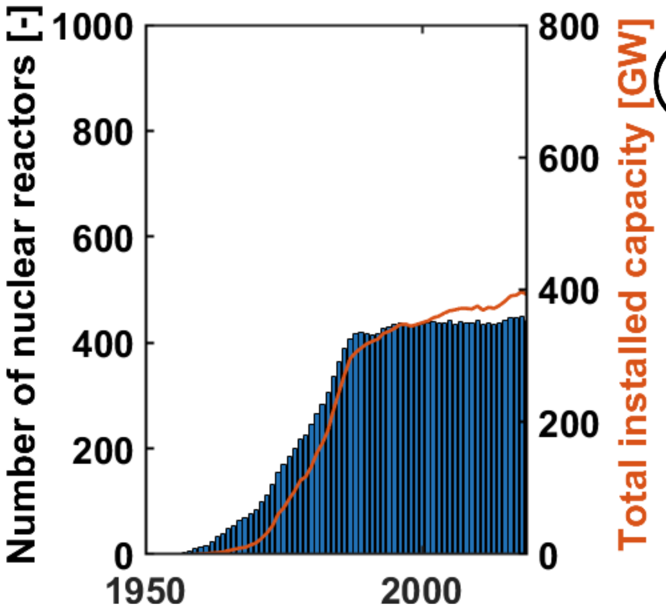

Data from [IAEA, 2021].

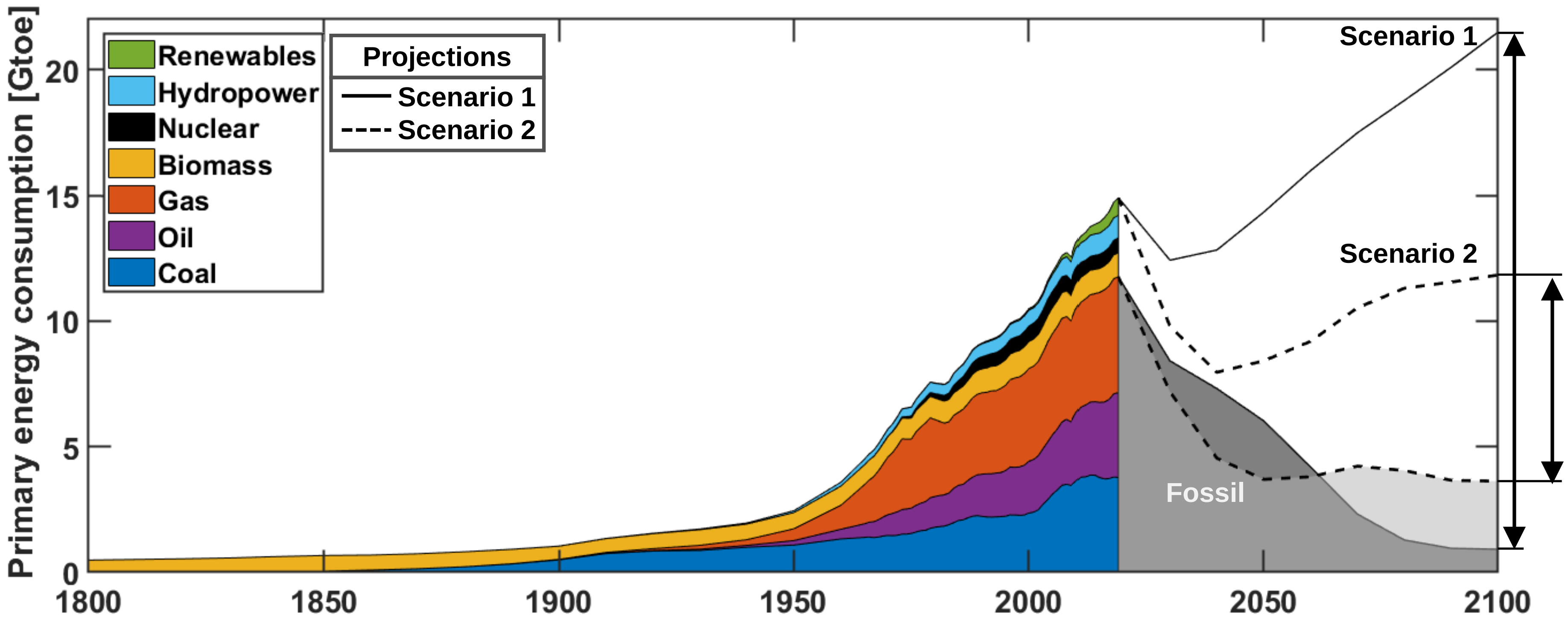

Data from [BP, 2022] & [Smil, 2016].

A story of energy

LIÈGE université
Urban & Environmental Engineering

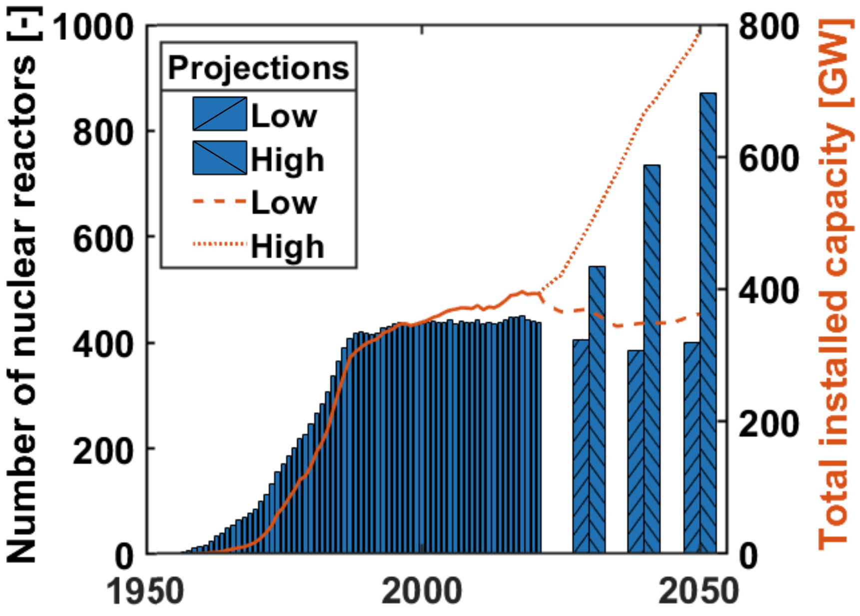

Data from [IAEA, 2021].

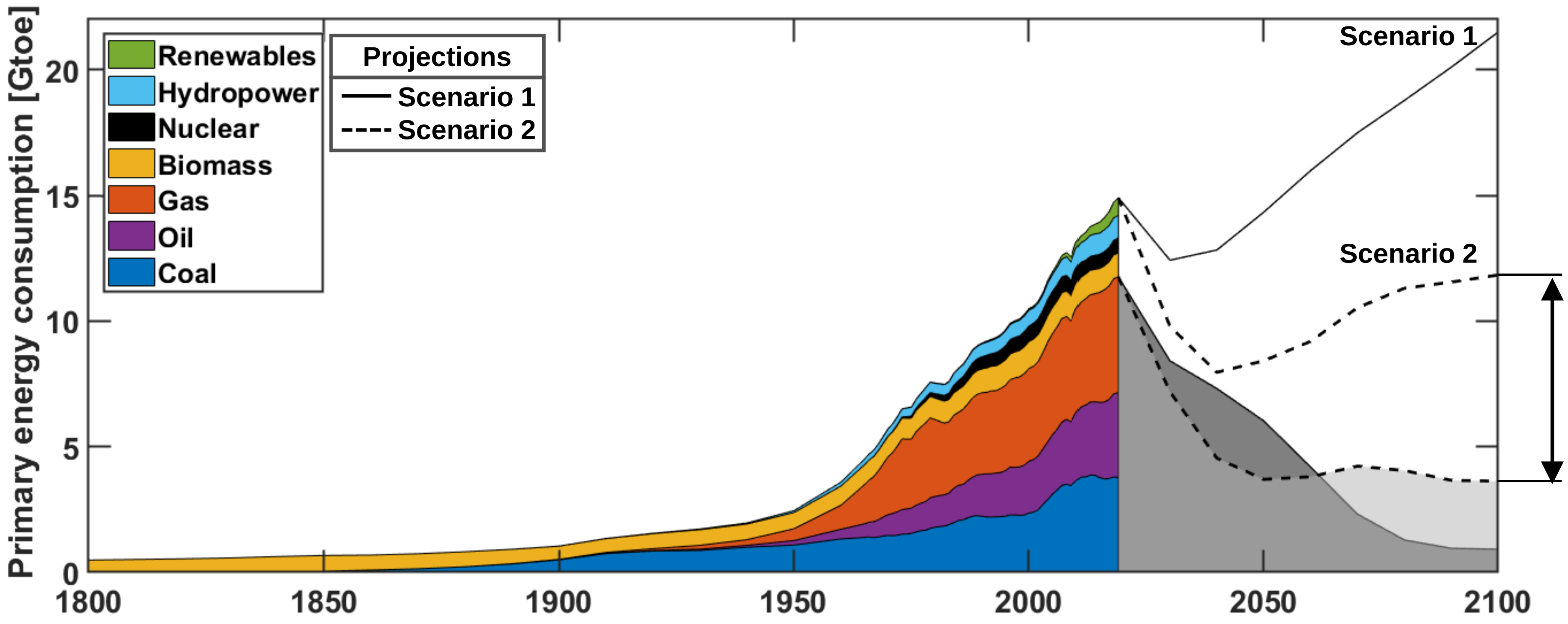

Data from [BP, 2022] & [Smil, 2016].

Management of radioactive waste

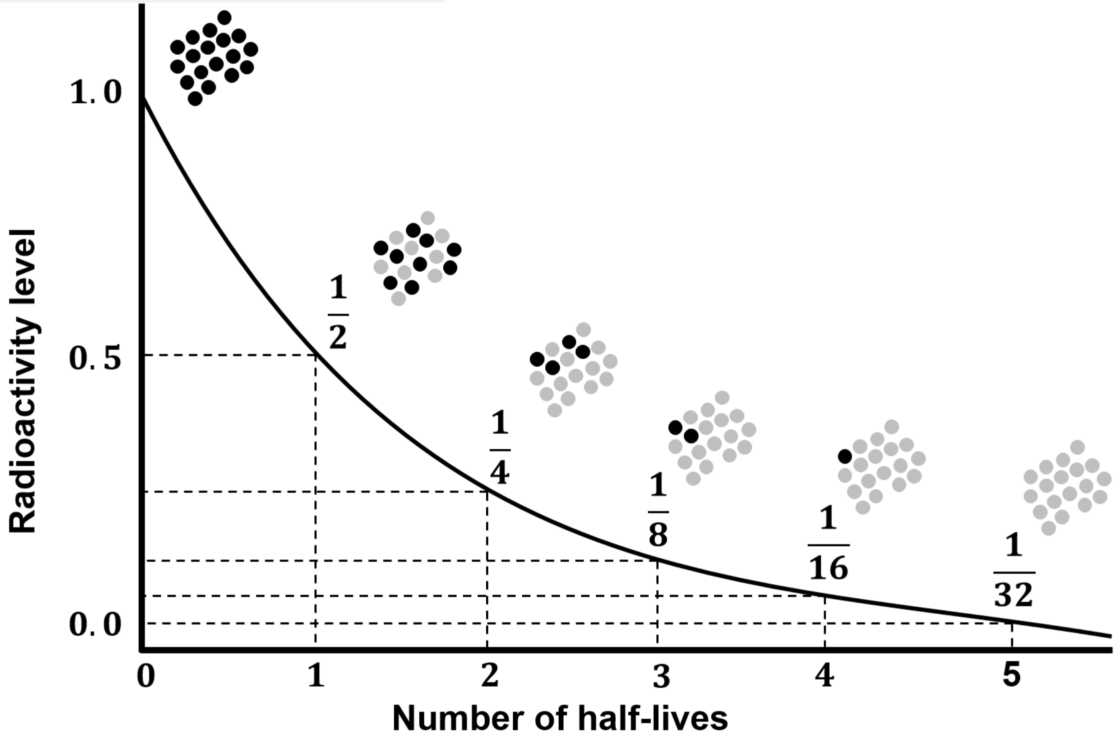

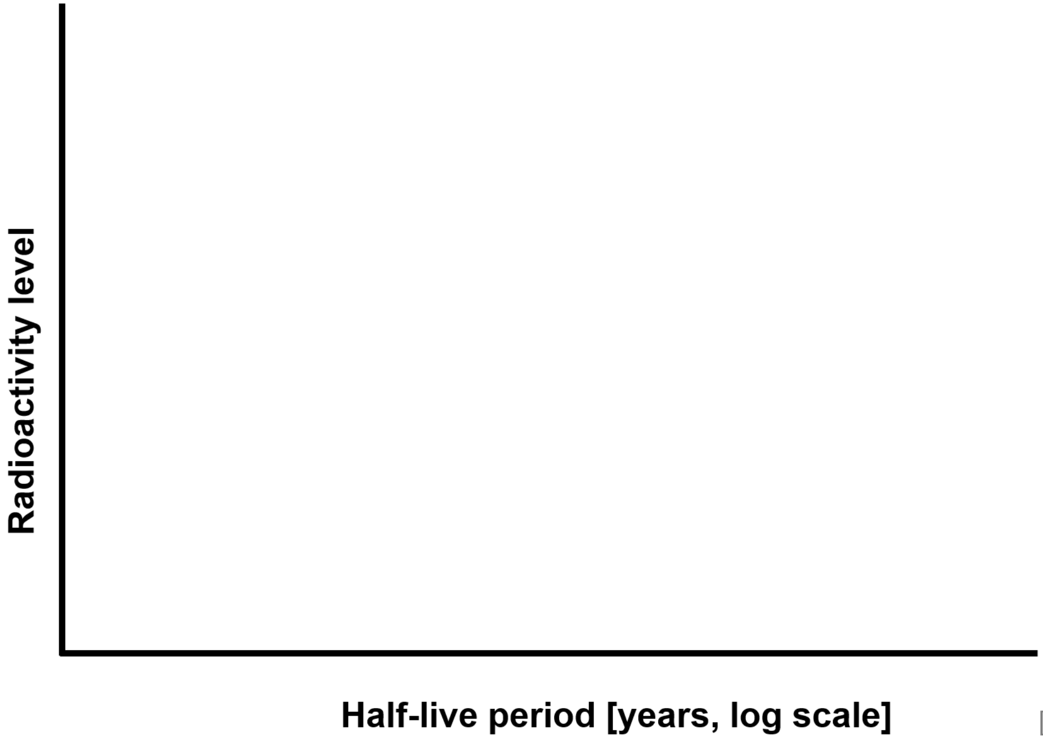

[IAEA, 2009].

Management of radioactive waste

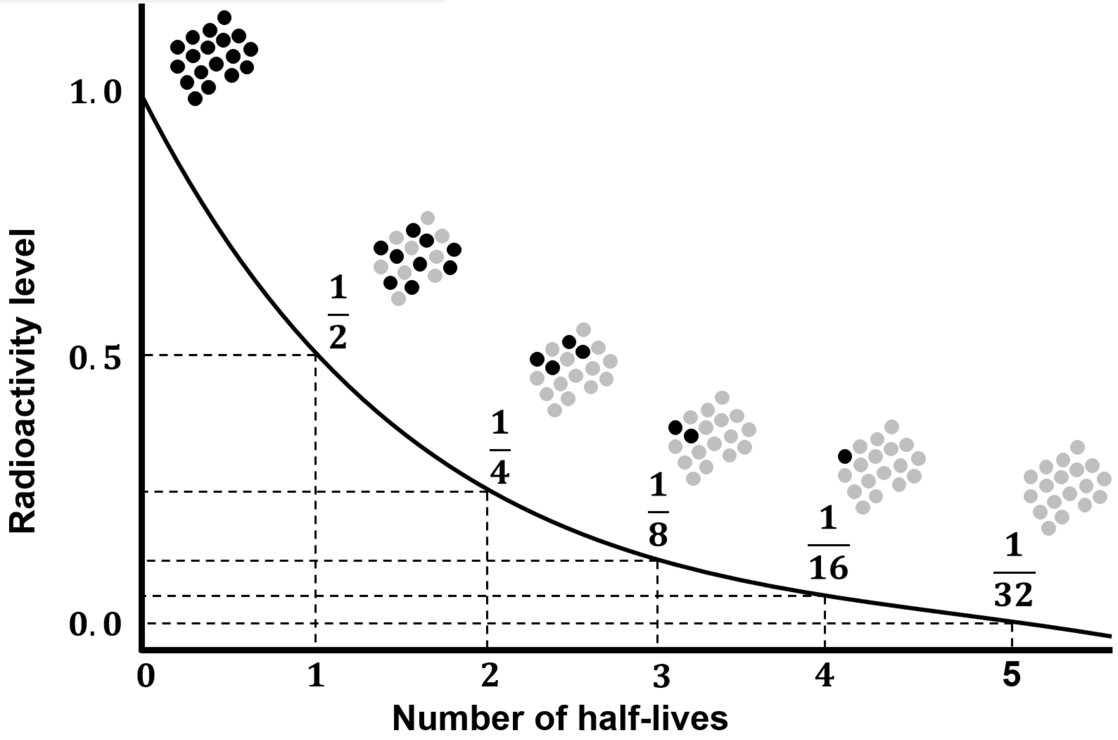

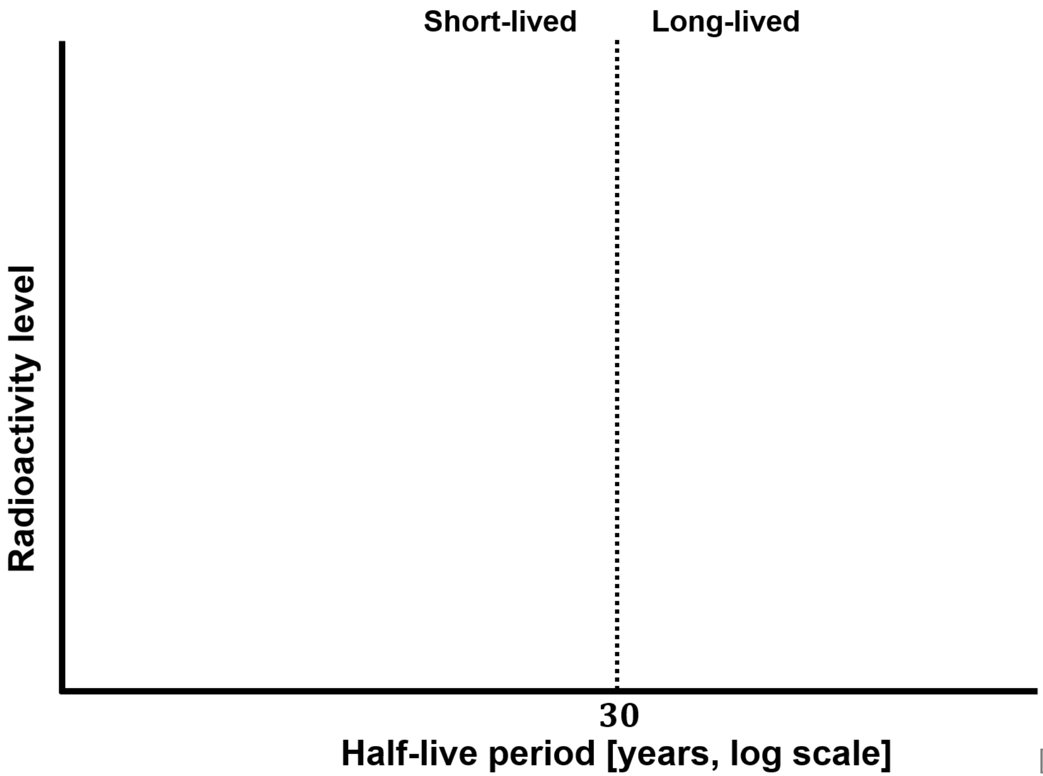

[IAEA, 2009].

Management of radioactive waste

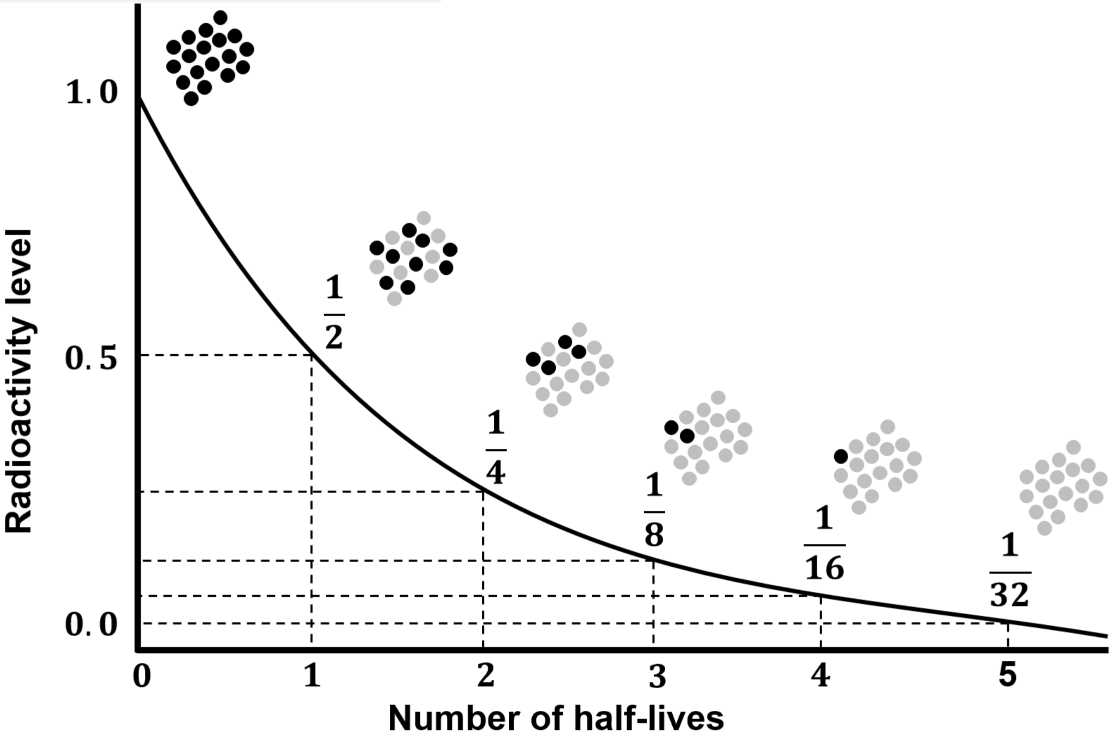

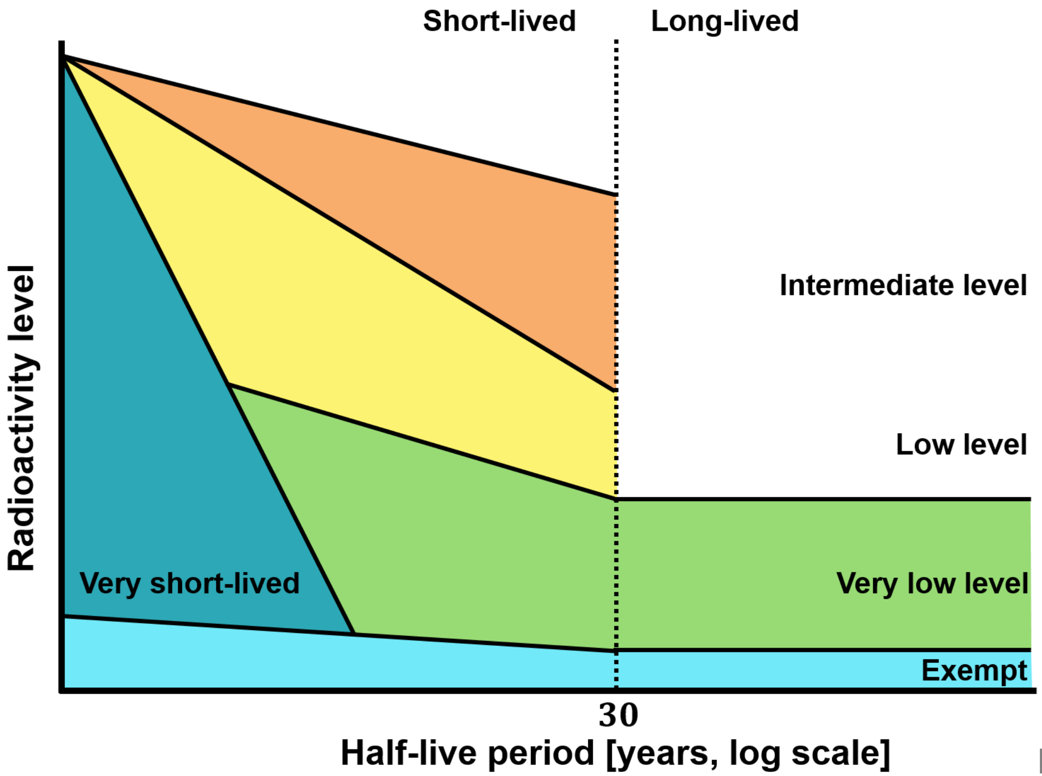

[IAEA, 2009].

Management of radioactive waste

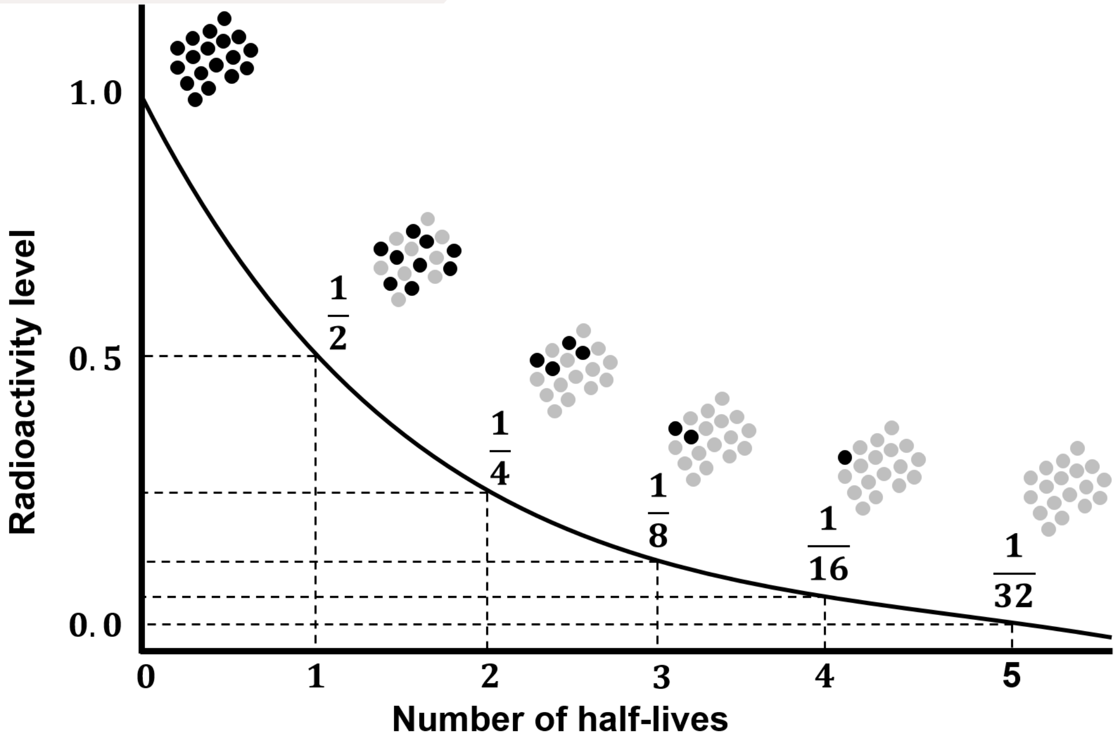

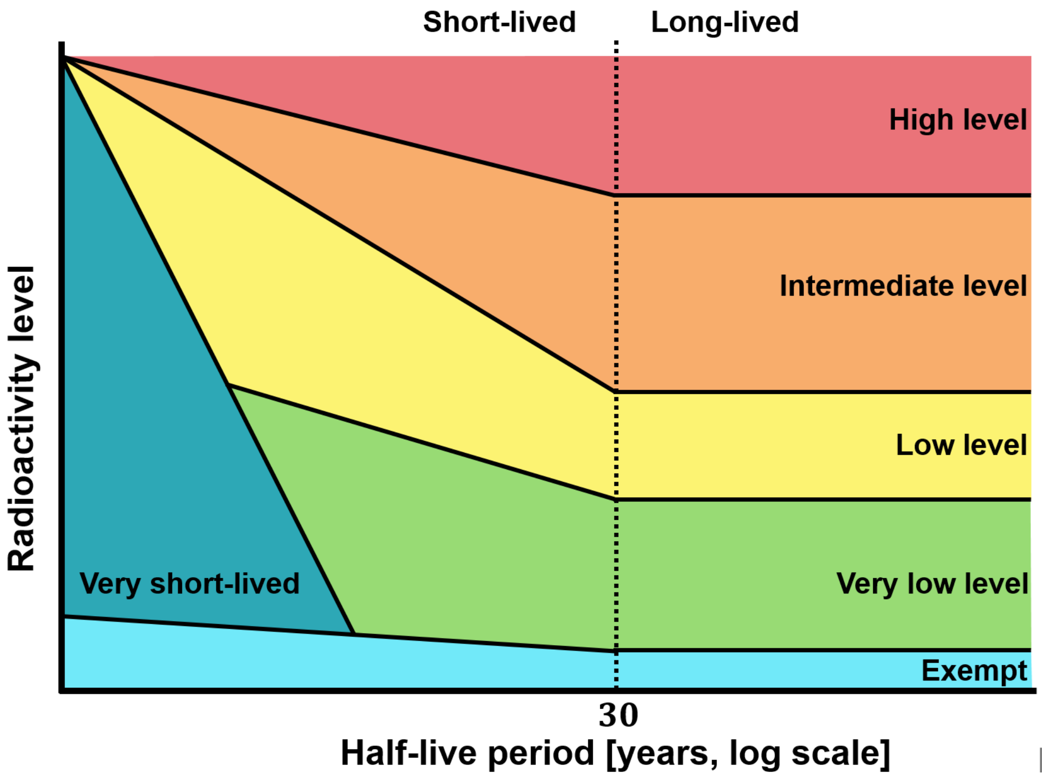

[IAEA, 2009].

Management of radioactive waste

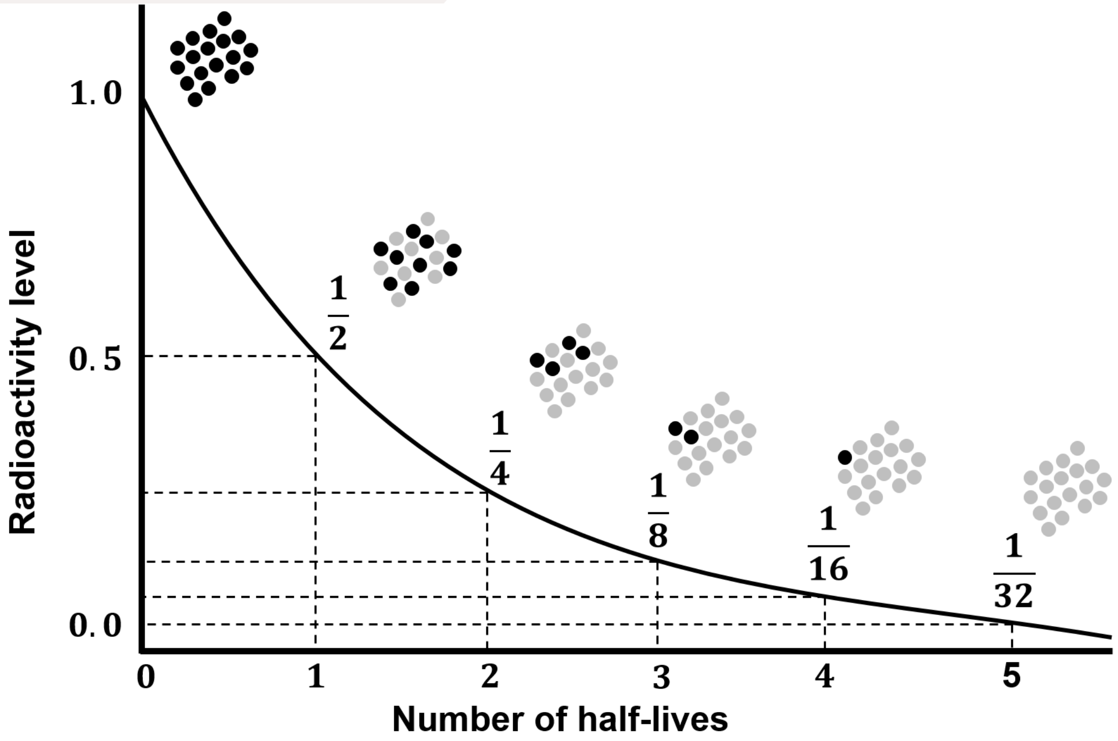

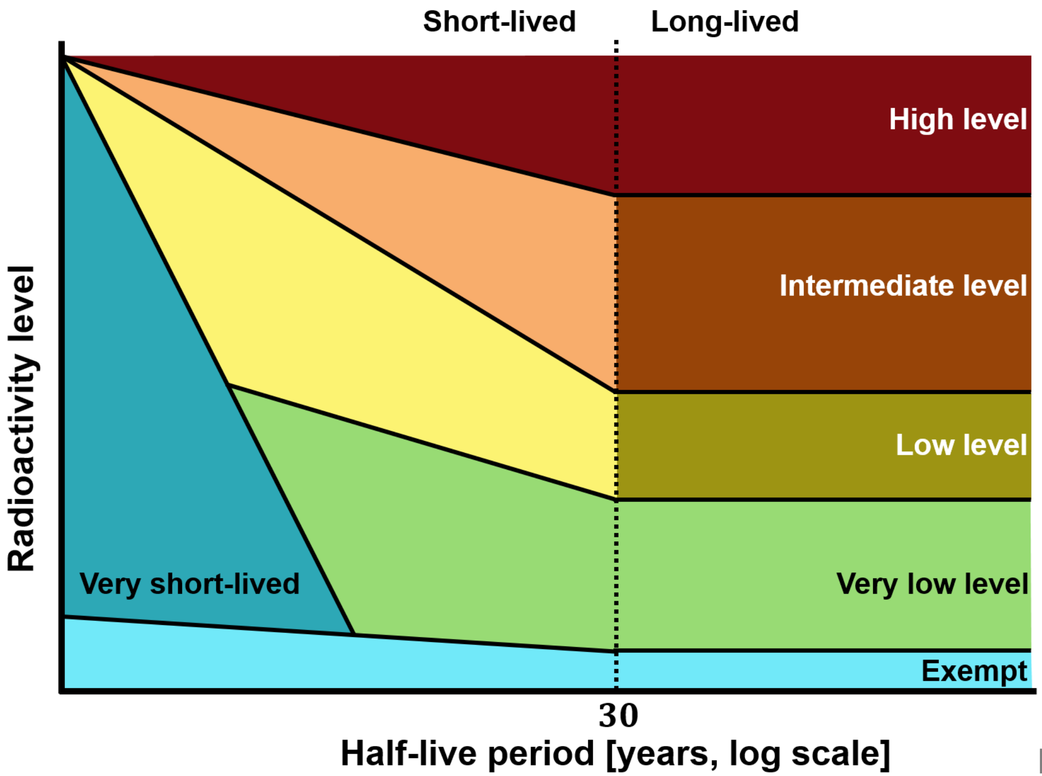

[IAEA, 2009].

LIÈGE université
Urban & Environmental Engineering

Table of Contents

Context
Nuclear electricity

Geological repository
Underground structure

Numerical Approach
Second gradient model

Application
Underground nuclear waste disposal

Deep geological repository

Intermediate
(long-lived)
&
high activity
wastes

Deep geological disposal

Repository in deep geological media with good confining properties

(Low permeability $K<10^{-12}$ m/s)

Underground structures

= network of galleries

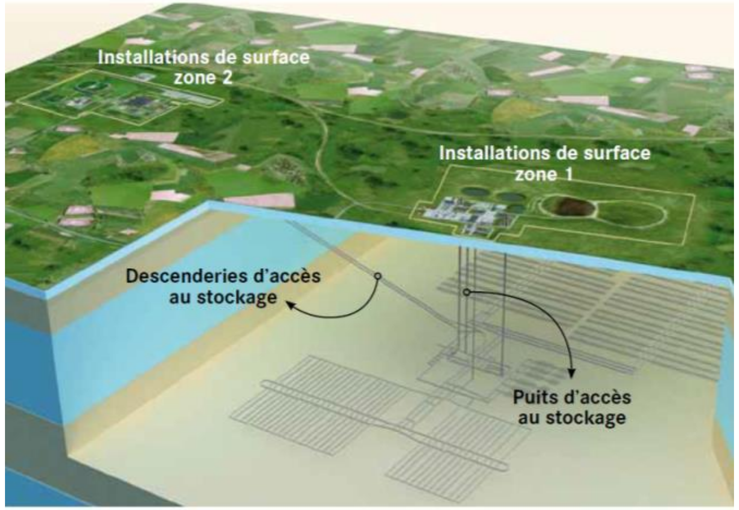

Deep geological repository

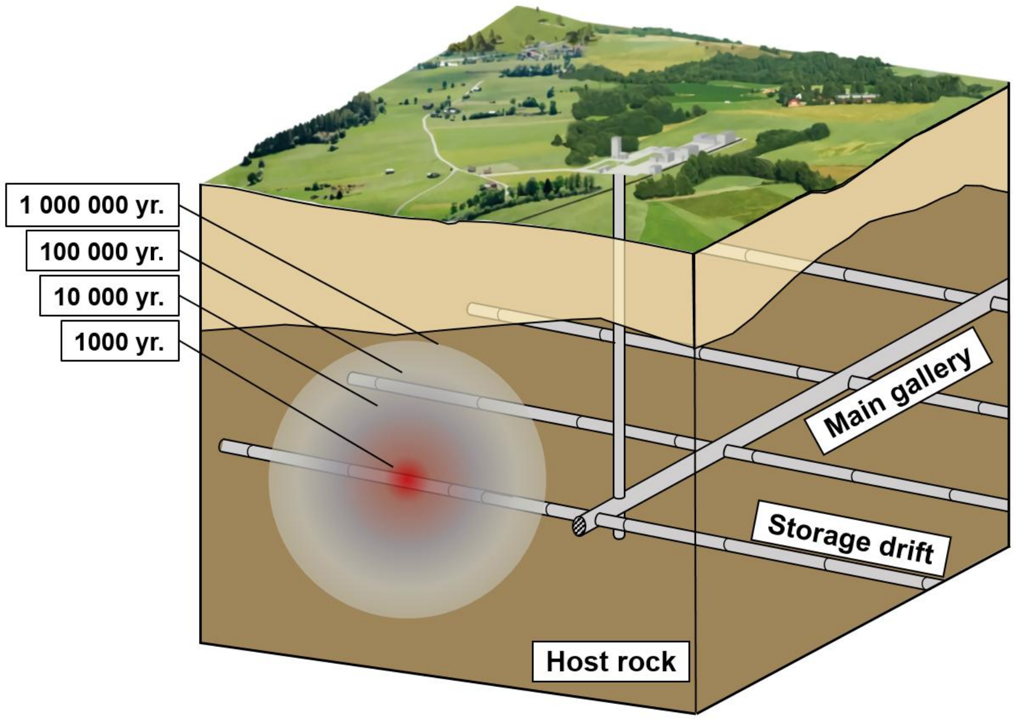

[ENSI/IFSN, 2021].

Deep geological repository

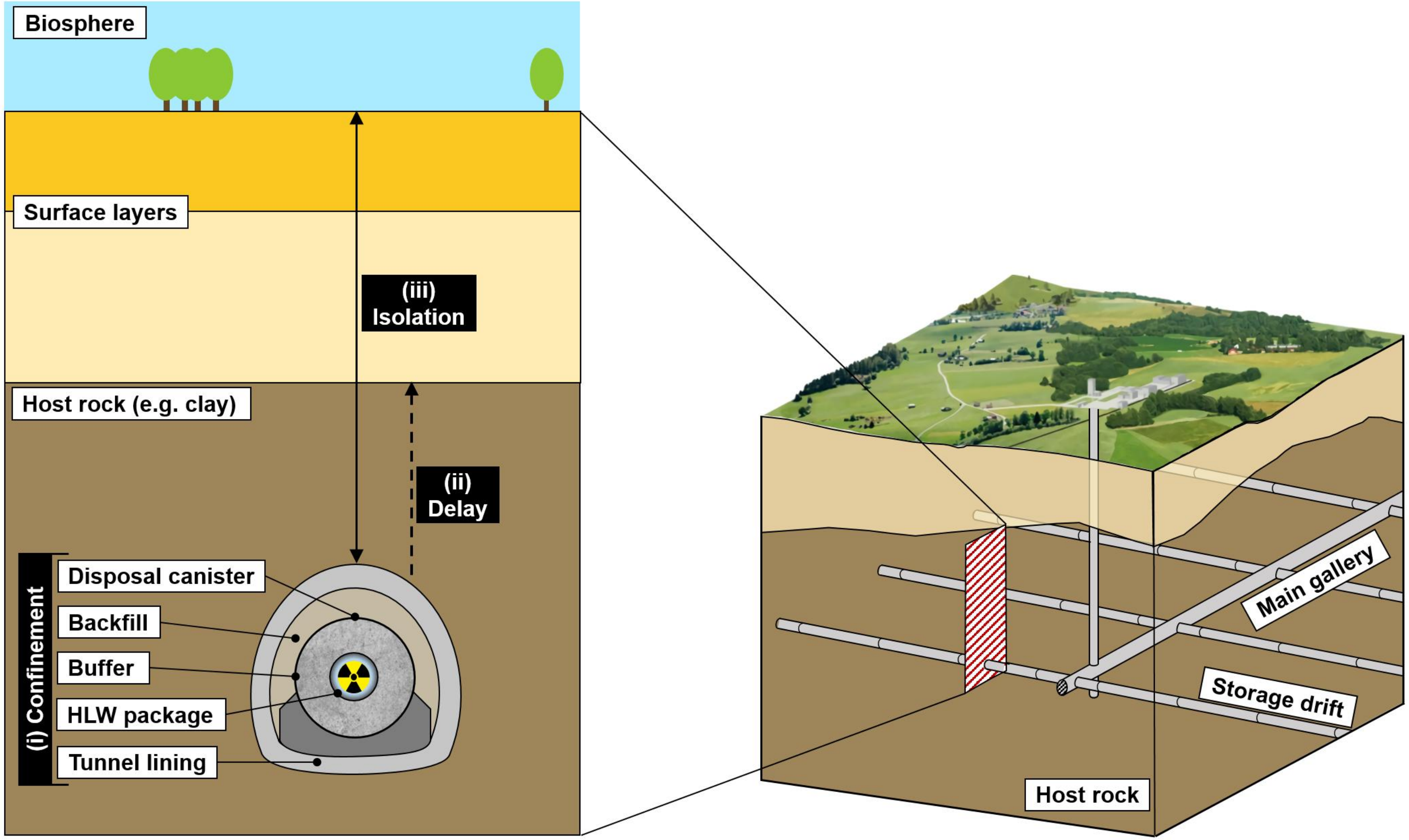

[ENSI/IFSN, 2021].

Deep geological repository

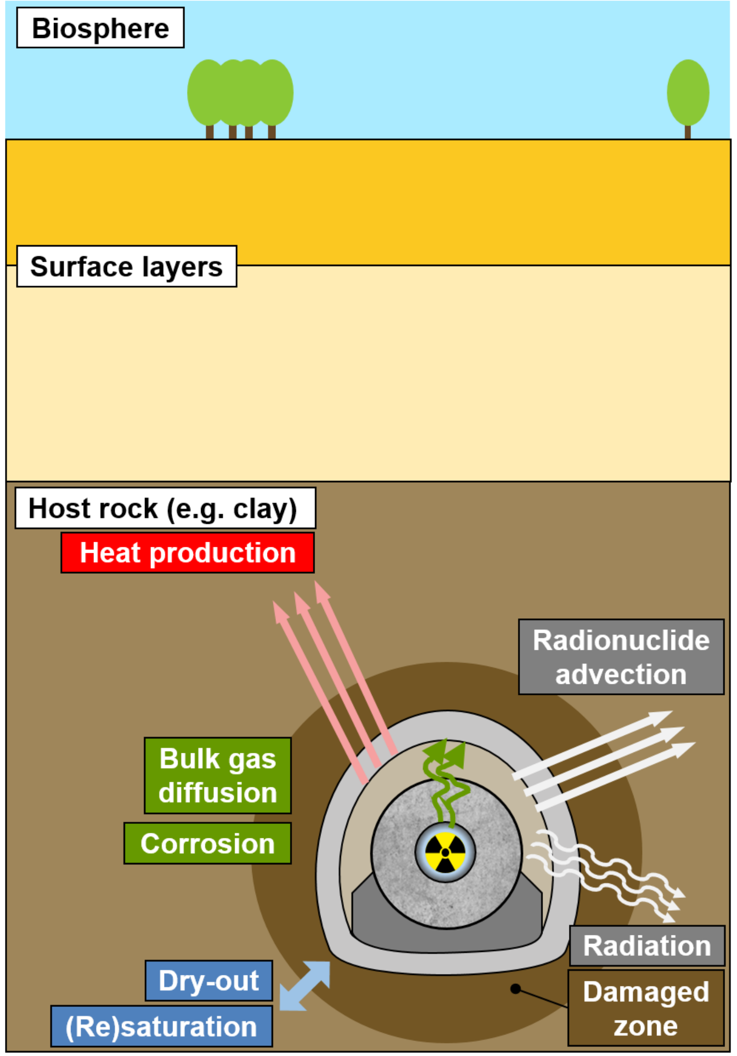

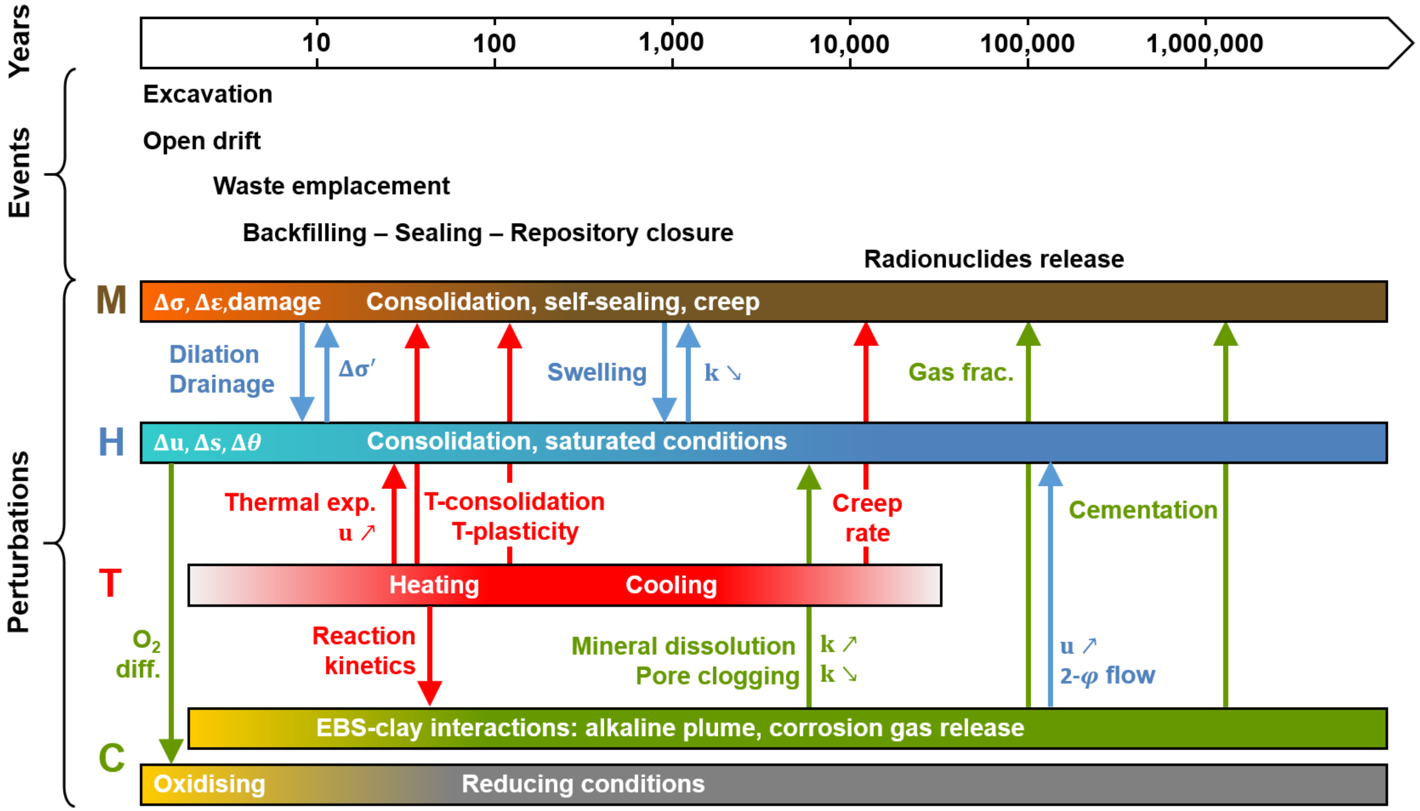

[Sillen, 2012].

Long term management of radioactive wastes

Callovo-Oxfordian claystone (COx)

Sedimentary clay rock (France).

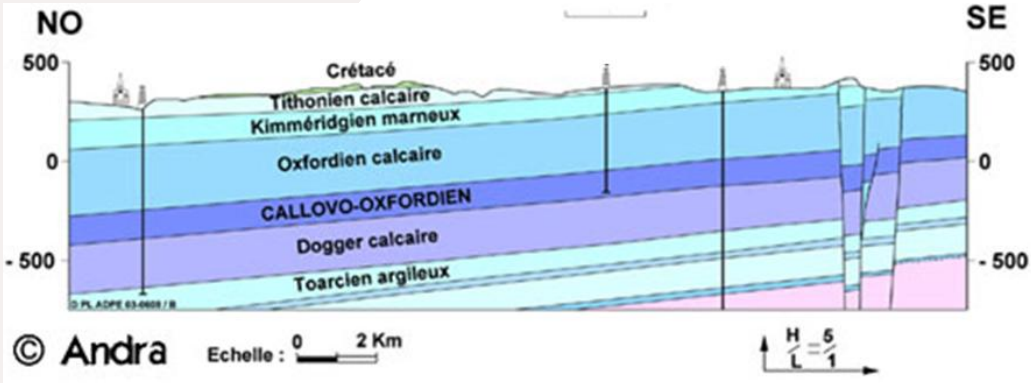

Borehole core samples
(Andra, 2005)

- Underground research laboratory

Feasibility of a safe repository

France (Meuse / Haute-Marne, Bure)

(Armand et al., 2014)

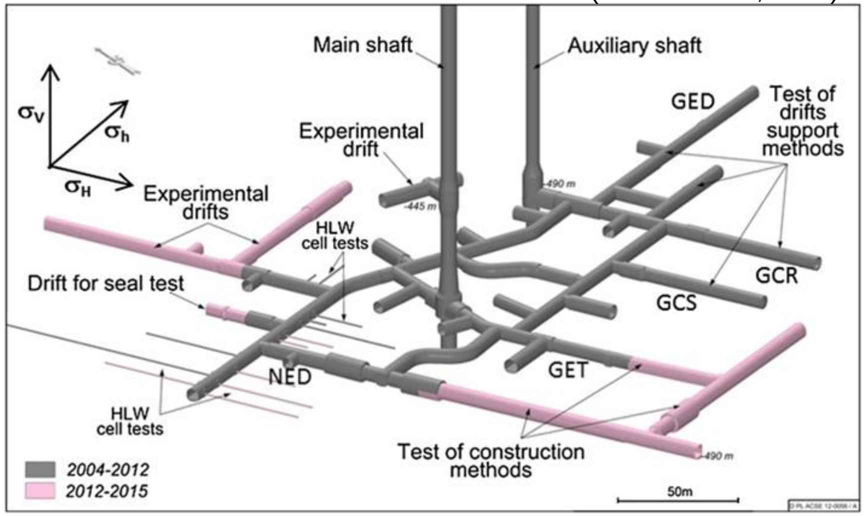

Repository phases

Time

Construction
→ Excavation

Maintenance
→ Ventilation

Repository
→ Sealing

Long term
→ Corrosion, heat generation

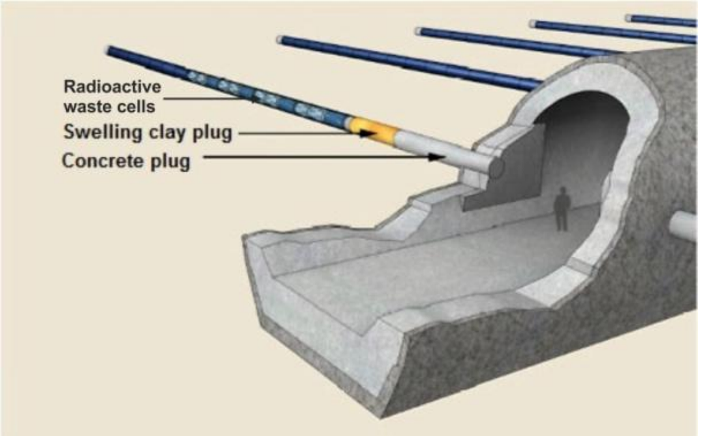

Type C wastes (Andra, 2005)

THM COUPLINGS

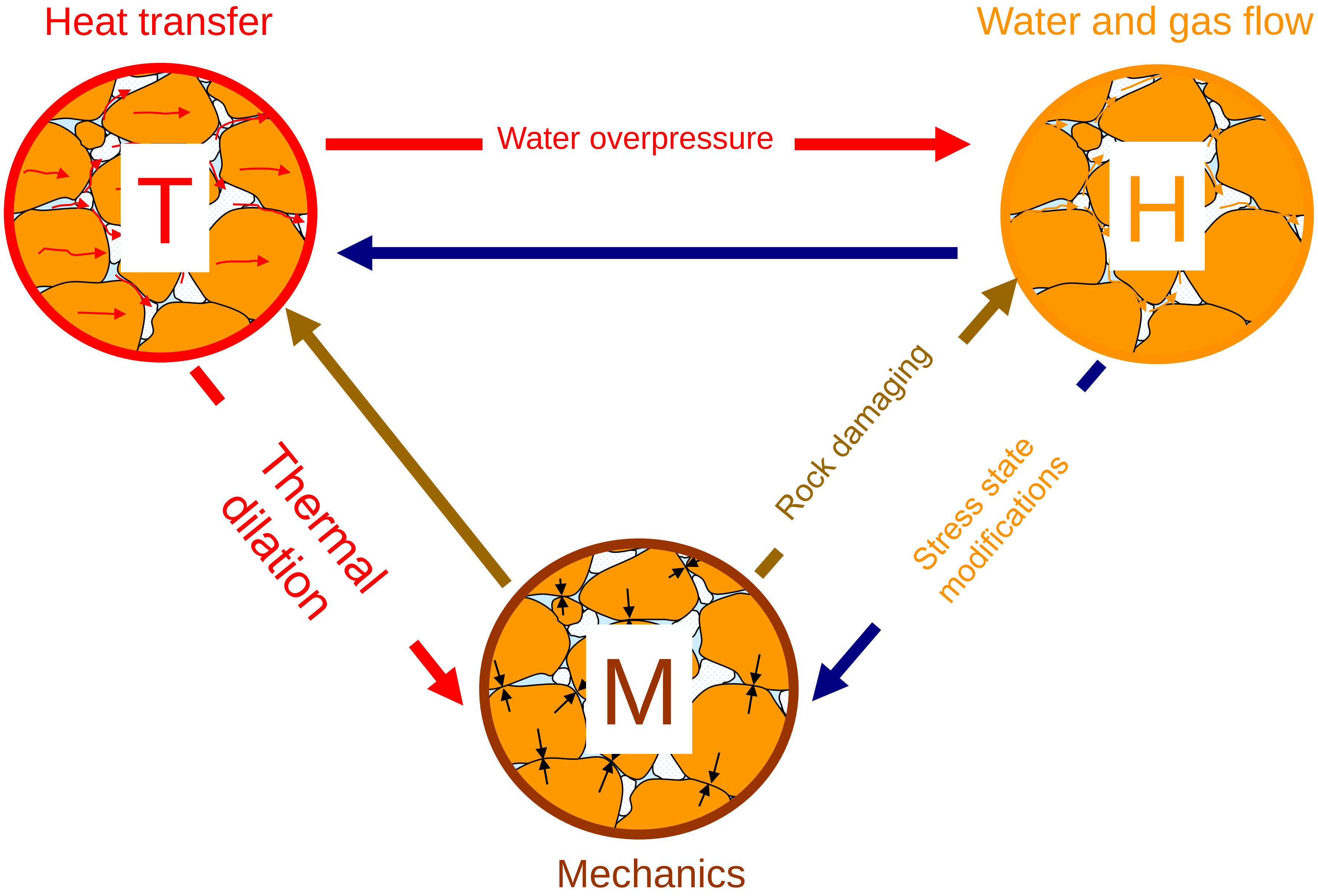

Repository phases

LIÈGE université Urban & Environmental Engineering

Time

Construction
→ Excavation

Maintenance
→ Ventilation

Repository
→ Sealing

Long term
→ Corrosion, heat generation

Type C wastes (Andra, 2005)

Excavated damaged zone - EDZ

Construction

Mechanical fracturing

Excavation

↓

Stress redistribution

↓

Damage / Fracturing

↓

Coupled processes
HM property modifications

↓

Safety function alteration

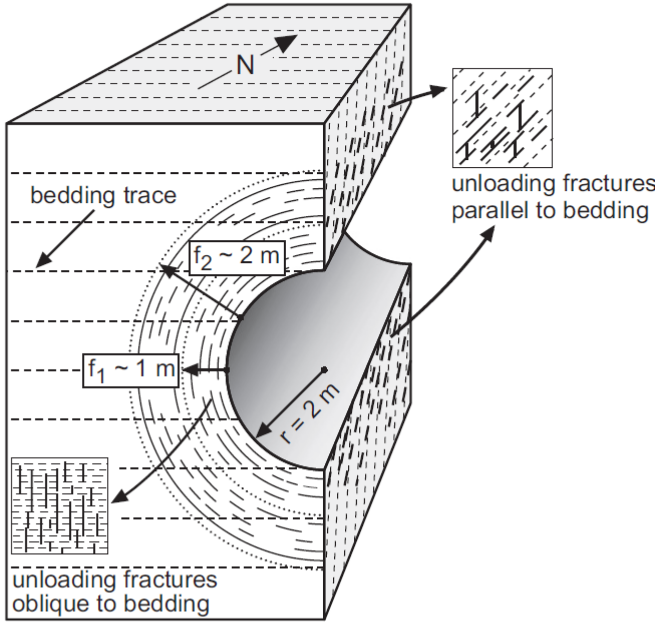

Fracturing & permeability increase
(several orders of magnitude)

Opalinus clay in Switzerland
(Bossart et al., 2002)

Maintenance

Water transfer

Galleries ventilation

↓

Air-rock interaction

↓

Drainage / desaturation

↓

Modification of the
water transfer

Excavated damaged zone - EDZ

Construction
Mechanical fracturing

Excavation
↓
Stress redistribution
↓
Damage / Fracturing
↓
Coupled processes
HM property modifications
↓
Safety function alteration

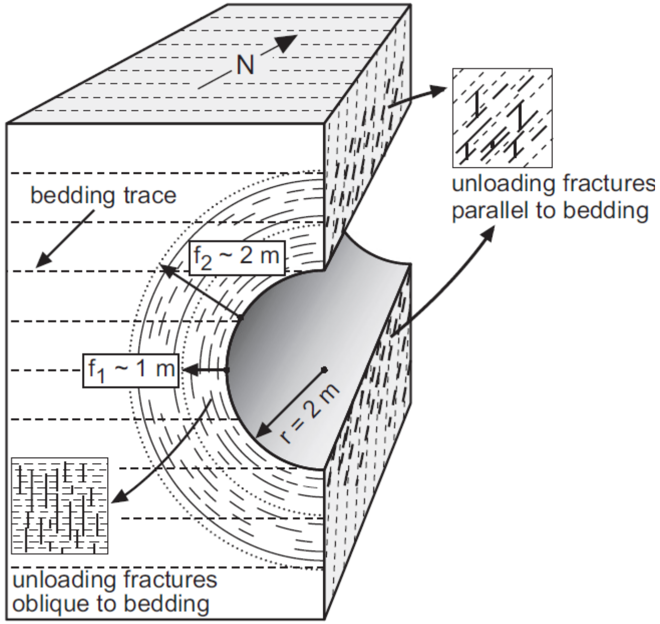

Fracturing & permeability increase
(several orders of magnitude)

Opalinus clay in Switzerland
(Bossart et al., 2002)

Maintenance
Water transfer

Galleries ventilation
↓
Air-rock interaction
↓
Drainage / desaturation
↓
Modification of the water transfer

LIÈGE université
Urban & Environmental Engineering

Table of Contents

Fracturation observation

Anisotropies: - stress : $\sigma_H > \sigma_h \sim \sigma_v$

- material : HM cross-anisotropy.

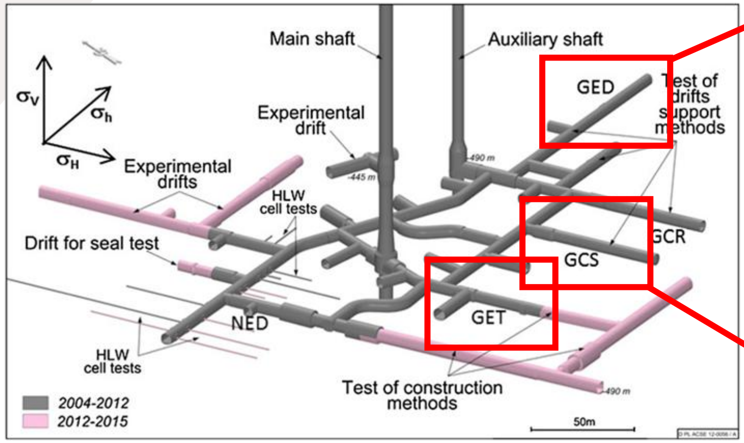

(Armand et al., 2014)

Galery // to σ_h

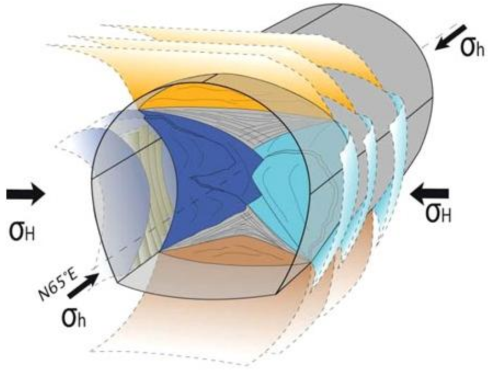

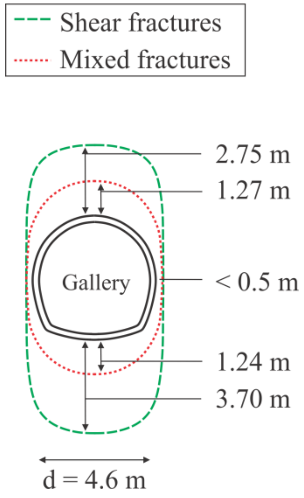

Galery // to σ_H

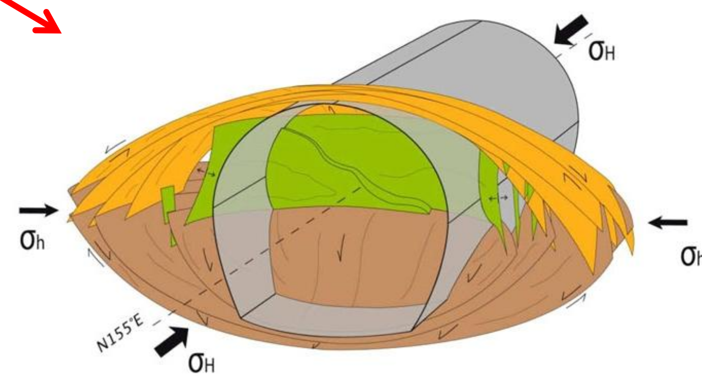

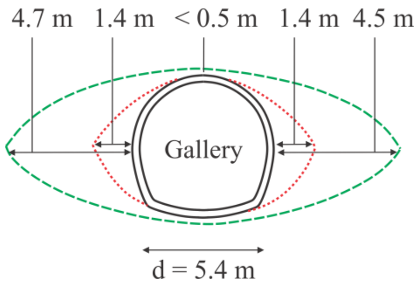

Issues: Prediction of the fracturing.
Effect of anisotropies ?
Permeability evolution & relation to fractures ?

Excavation / Fracturation modelling

Constitutive models for COx

- Mechanical law - 1st gradient model

Isotropic elasto-plastic internal friction model

Non-associated plasticity, Van Eeckelen yield surface :

$$F \equiv II_{\hat{\sigma}} - m\left(I_{\sigma'} + \frac{3\,c}{\tan\varphi_C}\right) = 0$$

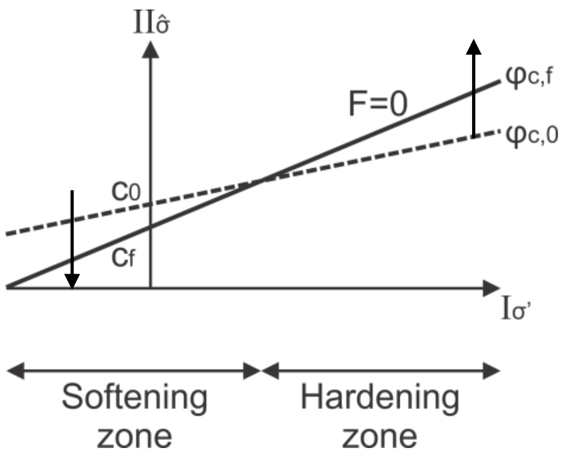

φ hardening / c softening

$$c = c_0 + \frac{\left(c_f - c_0\right)\hat{\varepsilon}^p_{eq}}{B_c + \hat{\varepsilon}^p_{eq}}$$

→ Strain localisation

- Hydraulic law

Fluid mass flow (advection, Darcy) : $$f_{w,i} = -\rho_w \frac{k_{w,ij}\,k_{r,w}}{\mu_w}\left(\frac{\partial p_w}{\partial x_j} + \rho_w\,g_j\right)$$

Water retention and permeability curves (Mualem - Van Genuchten's model)

Excavation / Fracturation modelling

Urban & Environmental Engineering

- Numerical model

HM modelling in 2D plane strain state

Gallery radius = 2.3 m

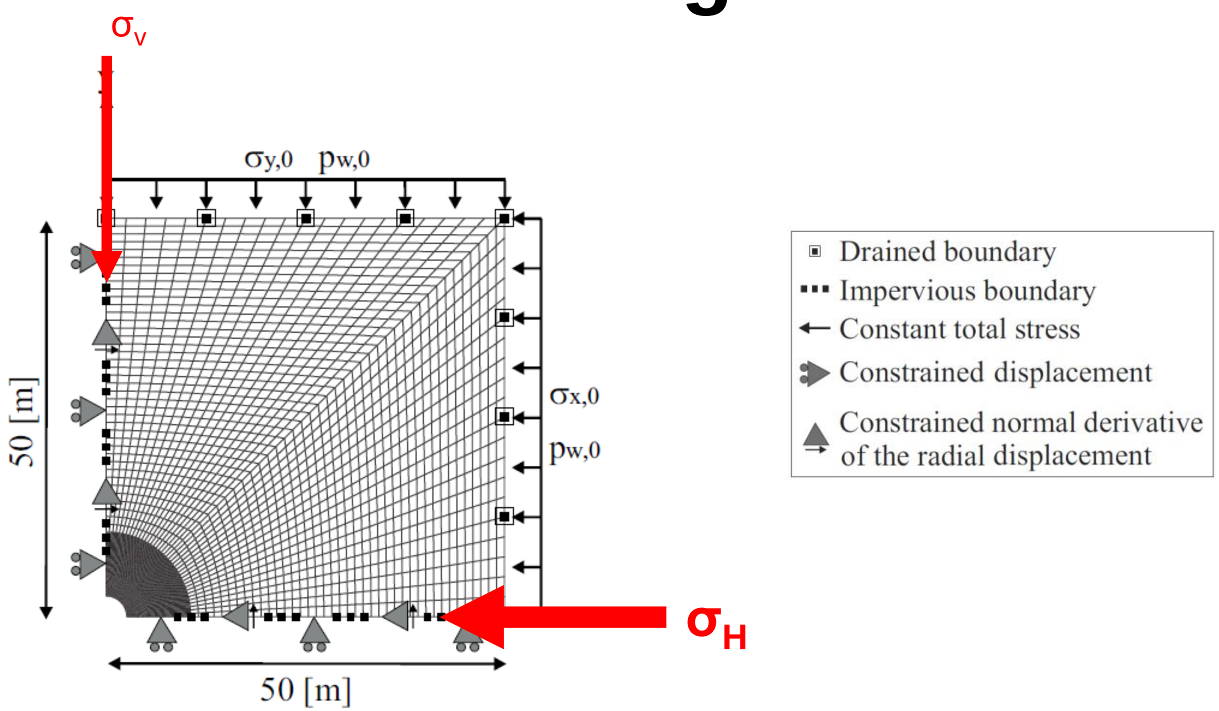

- Gallery in COx // σ_h

Effect of stress anisotropy

Anisotropic stress state

$p_{w,0}$ = 4.5 [MPa]

$\sigma_{x,0} = \sigma_H = 1.3\ \sigma_v$ = 15.6 [MPa]

$\sigma_{y,0} = \sigma_v$ = 12 [MPa]

$\sigma_{z,0} = \sigma_h$ = 12 [MPa]

- Excavation

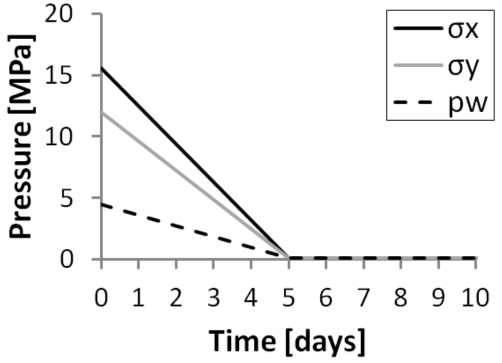

Excavation / Fracturation modelling

- Localisation zone

Incompressible solid grains, b=1

1009 days

End of excavation

Total deviatoric strain

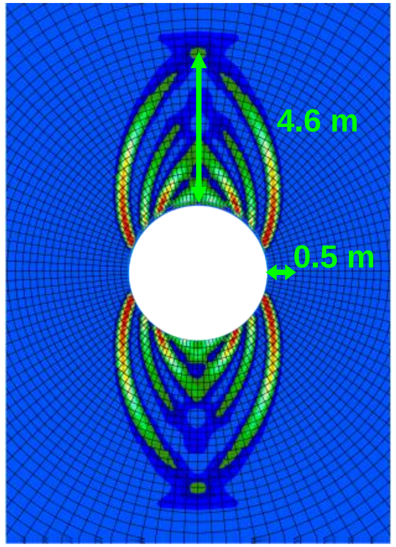

$$\hat{\varepsilon}_{eq} = \sqrt{\frac{2}{3}\hat{\varepsilon}_{ij}\hat{\varepsilon}_{ij}}$$

0 0.06

Plasticity

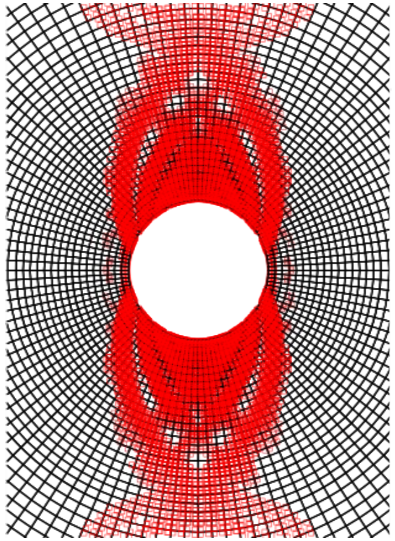

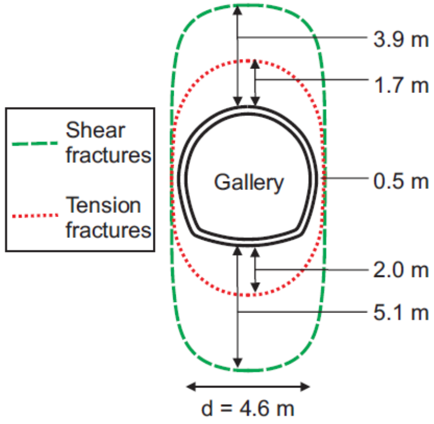

→ For an isotropic mechanical behaviour, the appearance and shape of the strain localisation are mainly due to mechanical effects linked to the anisotropic stress state.

Excavation / Fracturation modelling

LIÈGE université
Urban & Environmental Engineering

- Gallery air ventilation :

Water phases equilibrium at gallery wall (Kelvin's law)

$$RH = \frac{p_v}{p_{v,0}} = exp\left(\frac{-p_c\, M_v}{RT\, \rho_w}\right)$$

Compressibility of the solid grains: b=0.6

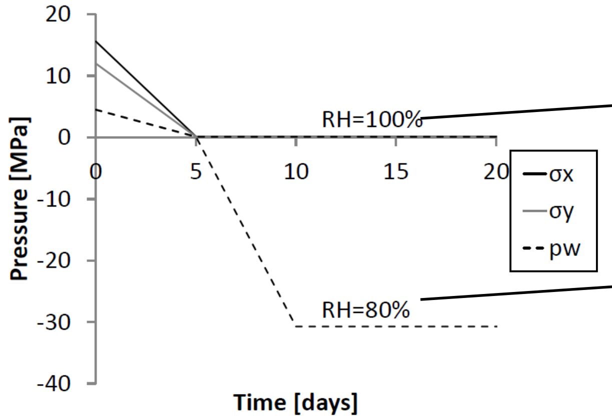

No ventilation
$p_w = p_{atm}$ [MPa]

Ventilation
p_w = -30.7 [MPa]

No ventilation | Ventilation

100 days | 1000 days | 100 days | 1000 days

Total deviatoric strain

0 0.184

Plasticity

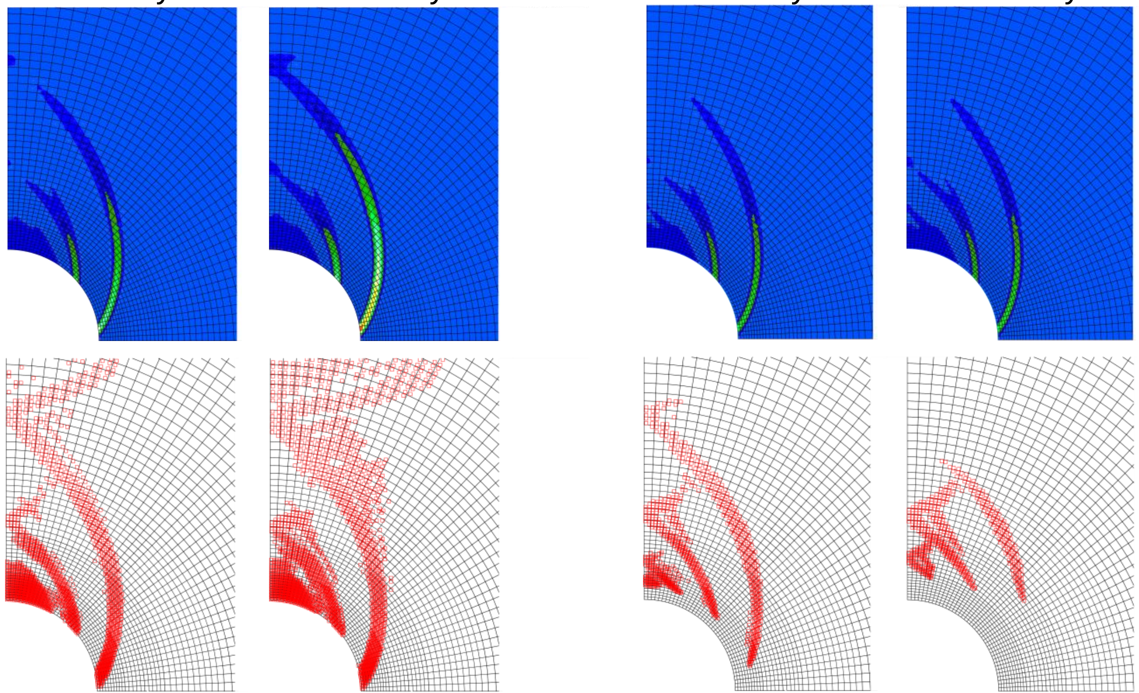

$$\sigma_{ij} = \sigma'_{ij} + b\, S_{r,w}\, p_w\, \delta_{ij}$$

→ suction ↑

→ σ' ↑

→ Elastic unloading

→ Inhibition of localisation

→ Restrain ε

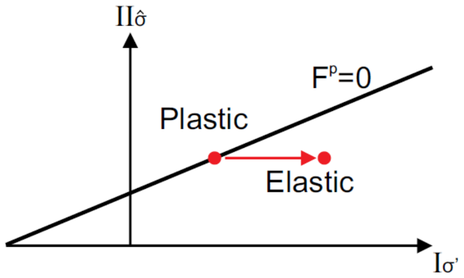

Excavation / Fracturation modelling

- Convergence:

Important during the excavation
Anisotropic convergence
Influence of the ventilation
Experimental results (GED - Andra's URL)
No strain localisation

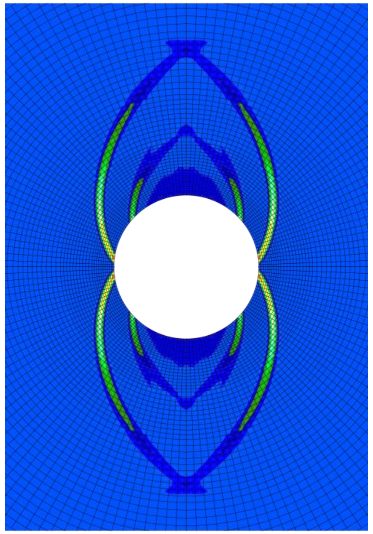

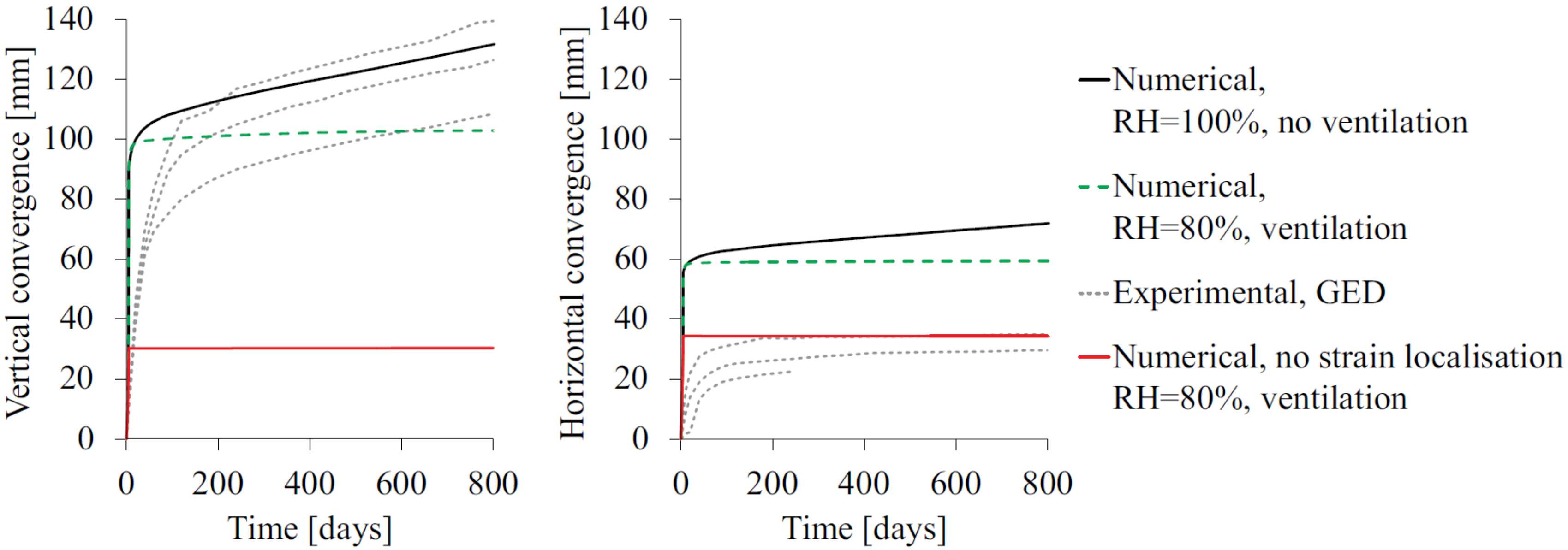

Excavation / Fracturation modelling

Conclusions and outlooks

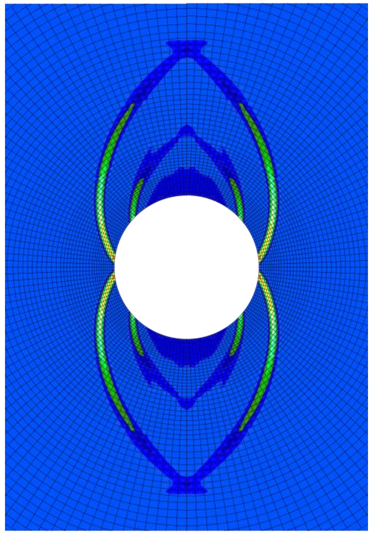

✓ Reproduction of EDZ with shear bands.

✓ Shape and extent of EDZ **governed by anisotropic stress state.**

- Next steps …

X Mechanical rock behaviour.

→ Material anisotropy, gallery // σ_H .

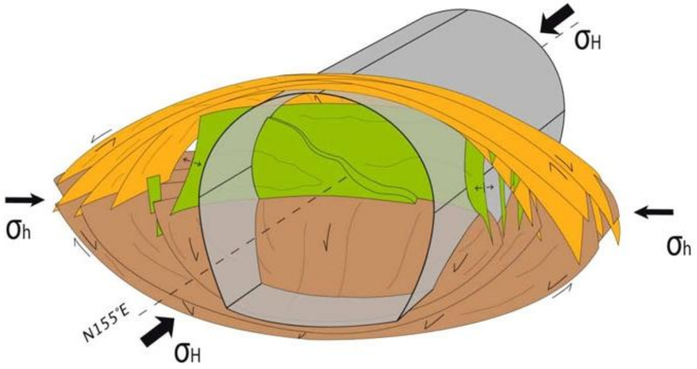

Excavation / Fracturation modelling

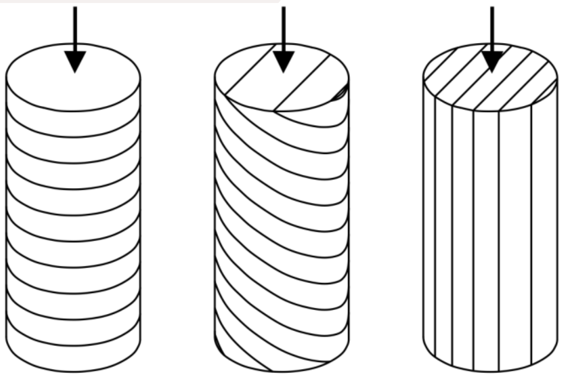

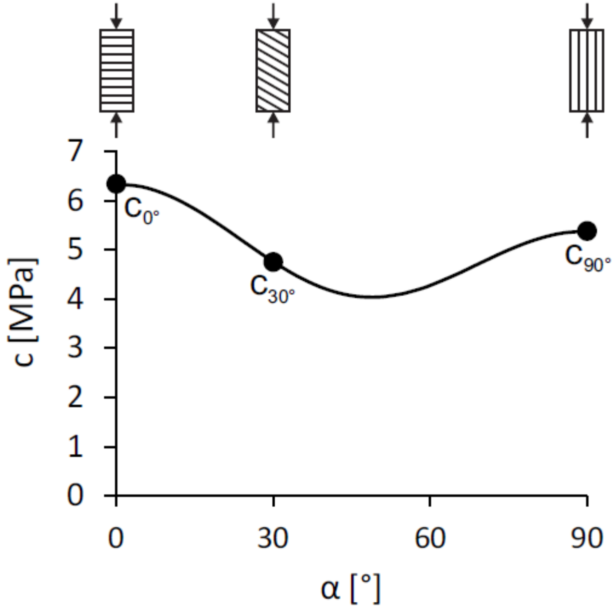

- Linear elasticity :

Cross-anisotropic (5 param.) + Biot's coefficients

$$E_{//}, E_{\perp}, \nu_{////}, \nu_{//\perp}, G_{//\perp} \qquad b_{//}, b_{\perp}$$

- Plasticity :

Cohesion anisotropy with fabric tensor

$$c_0 = a_{ij}\, l_i\, l_j \qquad l_i = \sqrt{\frac{\sigma_{i1}^{'2} + \sigma_{i2}^{'2} + \sigma_{i3}^{'2}}{\sigma_{ij}^{'}\sigma_{ij}^{'}}}$$

Cross-anisotropy

$$c_0 = \bar{c}\left(1 + A_{////}(1 - 3l_2^2) + b_1 A_{////}^2 (1 - 3l_2^2)^2 + \ldots\right)$$

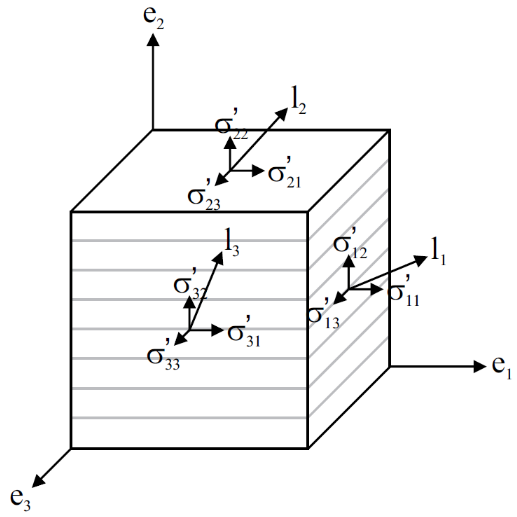

Excavation / Fracturation modelling

- Stress state

Major stress in the axial direction $\sigma_{x,0} = \sigma_h = 12.40$ MPa

Gallery // to σ_H $\sigma_{y,0} = \sigma_v = 12.70$ MPa

$\sigma_{z,0} = \sigma_H = 1.3 \times \sigma_h = 16.12$ MPa

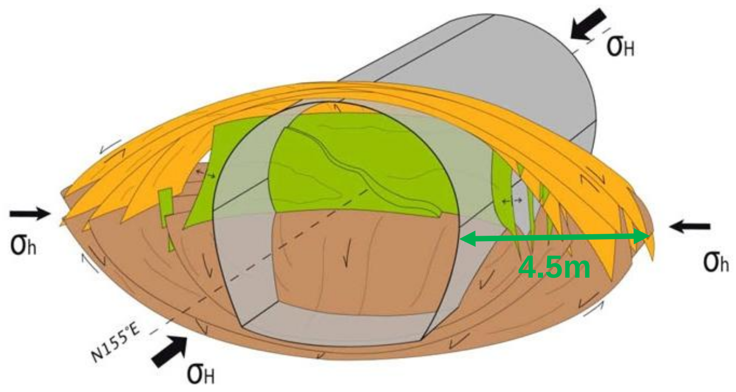

- Shear banding

Total deviatoric strain

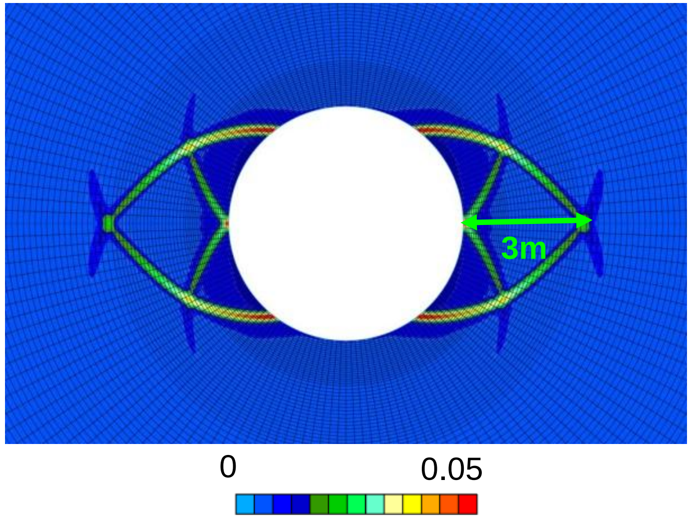

→ **Shape modification due to σ_H**

- Convergence

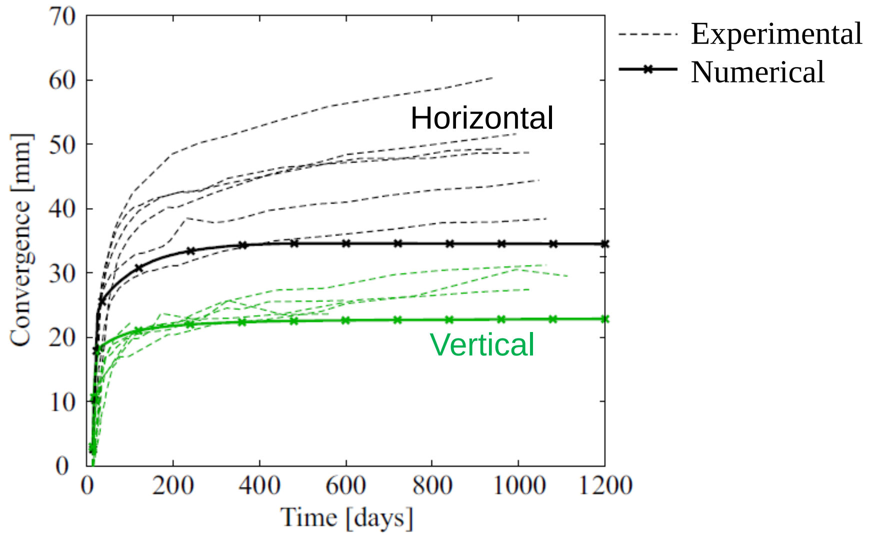

→ **Long-term deformation** → **Creep deformation**

Table of Contents

Geometry of the problem

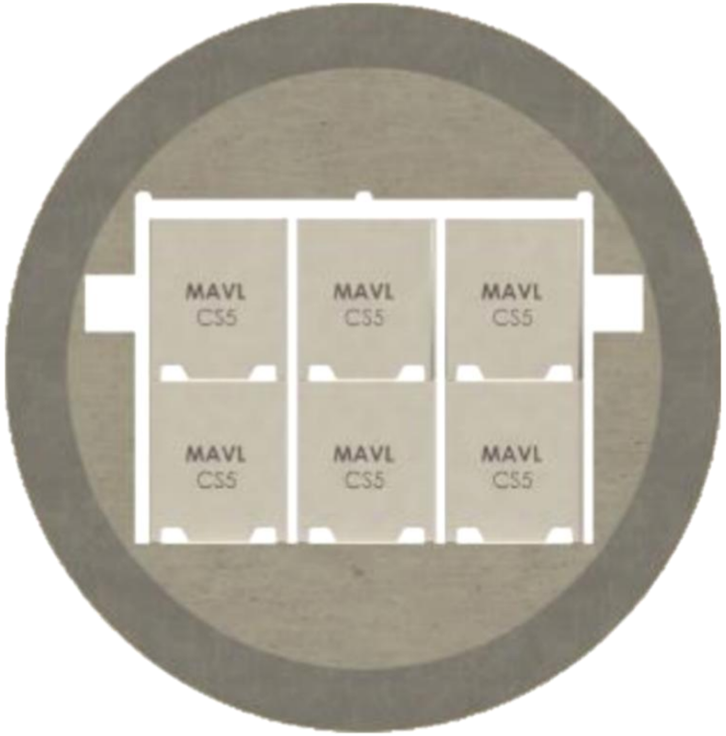

MAVL drift cross section

Geometry of the problem

Support structure

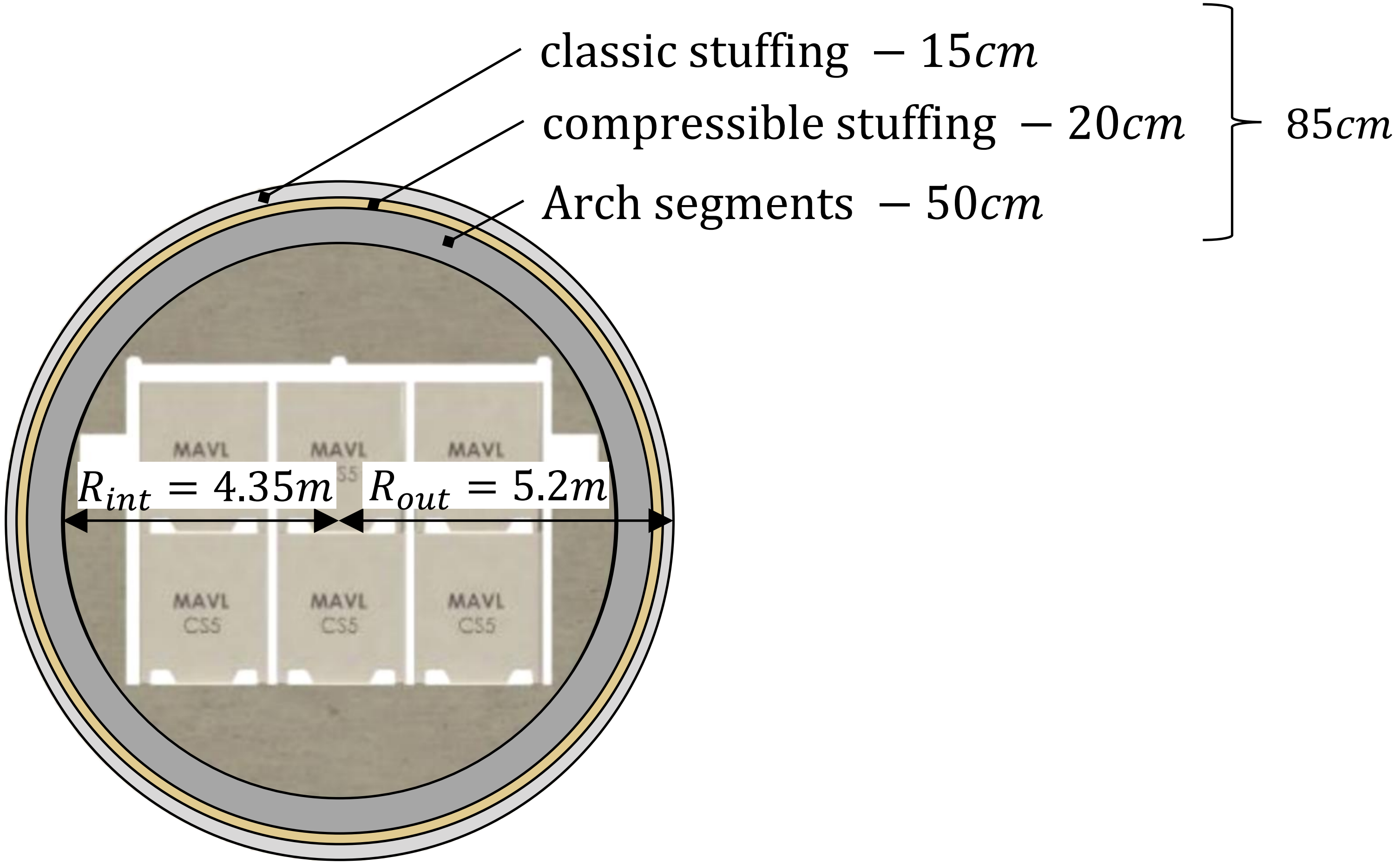

MAVL drift cross section

Geometry of the problem

Bedding planes orientation

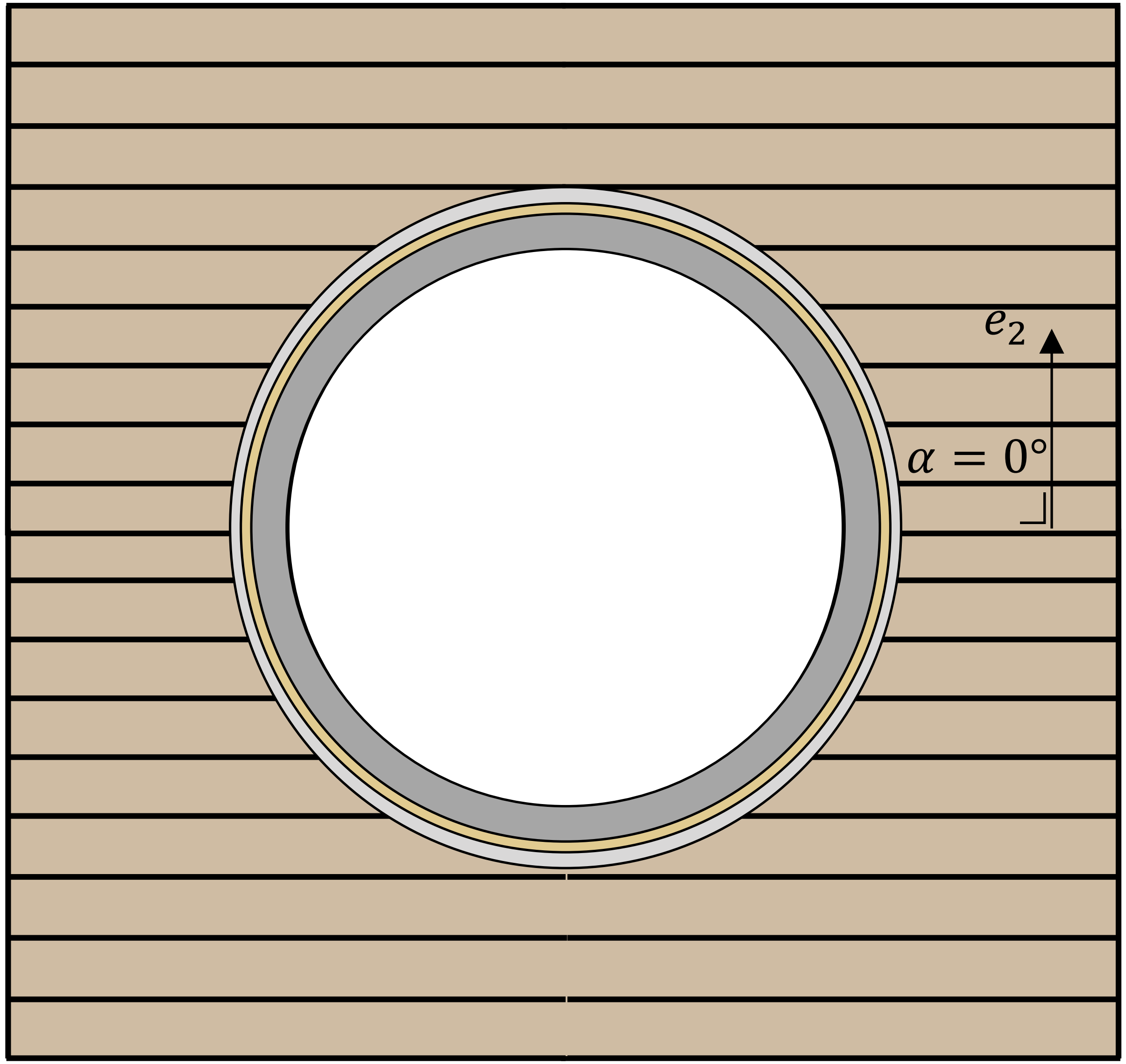

MAVL drift cross section

Modelling stages

Step 1 – Excavation (1 day)

- Initial step
- Drilling: - deconfinement of the rock mass
  - drained wall
  - constant gas pressure

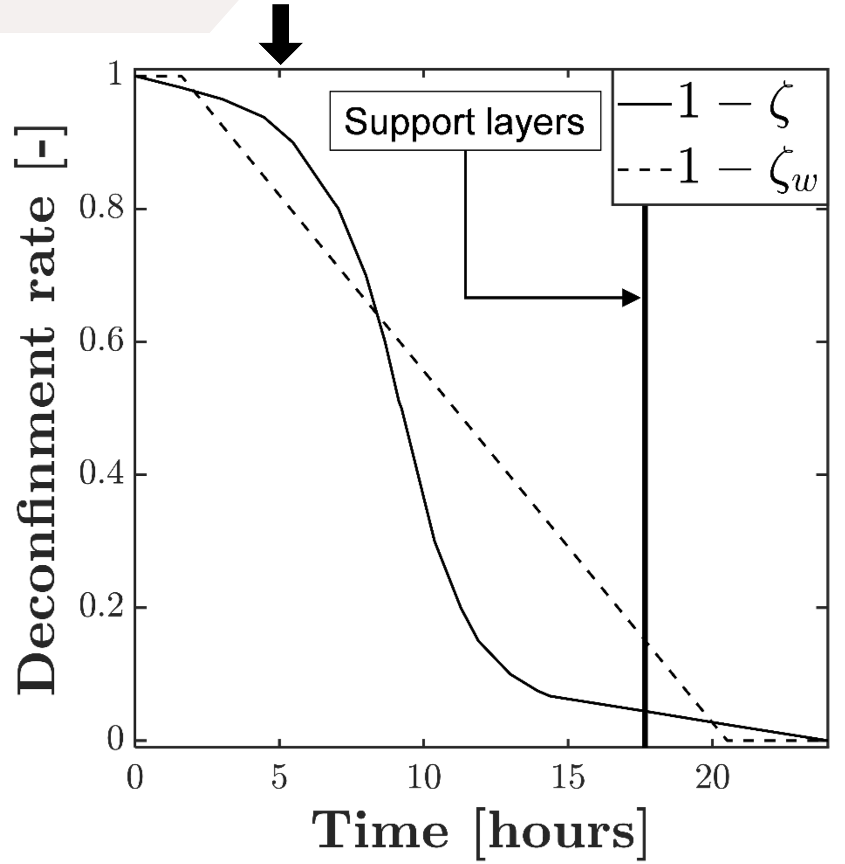

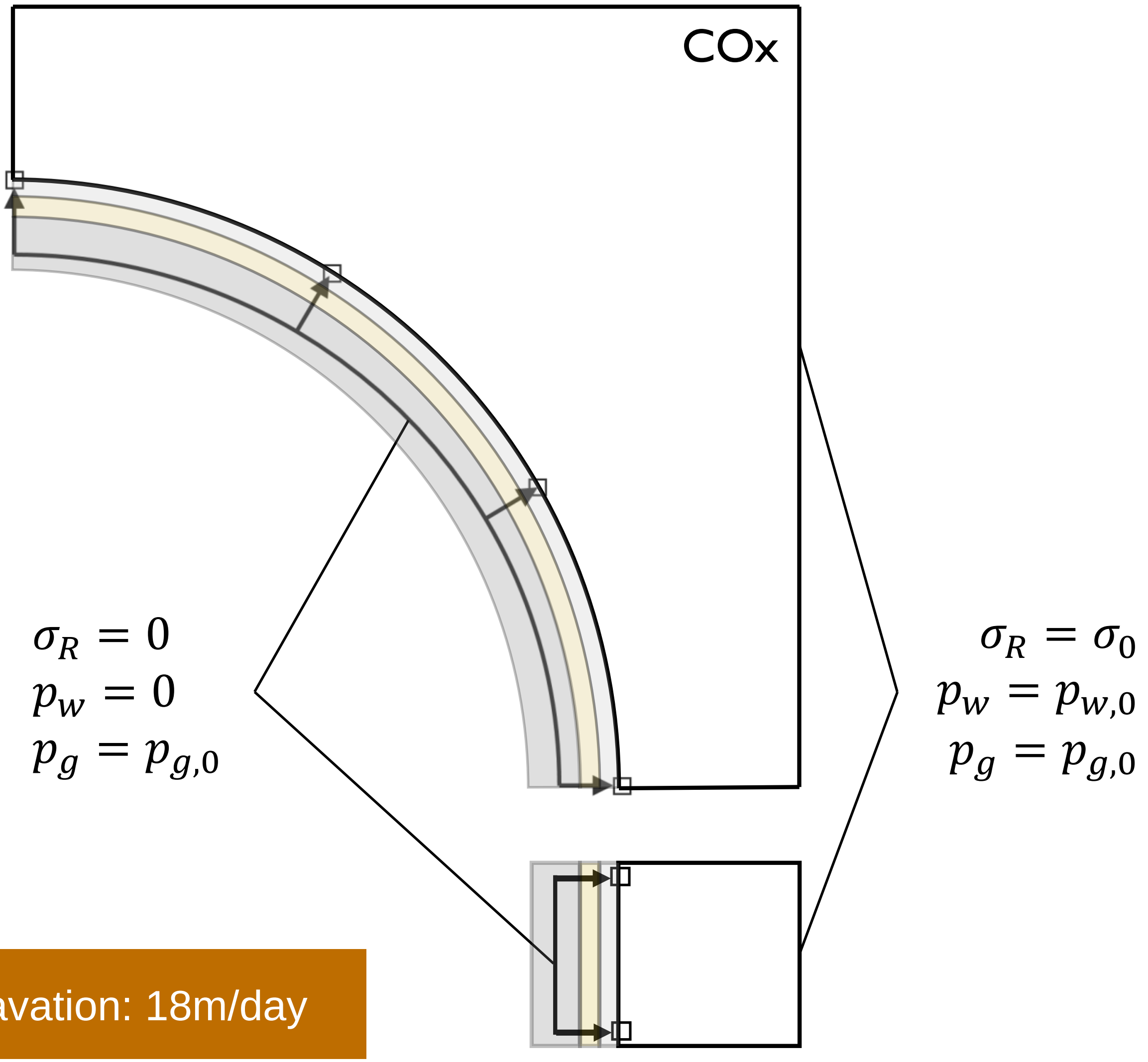

Rate of excavation: 18m/day

Modelling stages

Step 1 – Excavation (1 day)

- Initial step
- Drilling
- Activation of the supports: - stuffing layers
  - arch segments

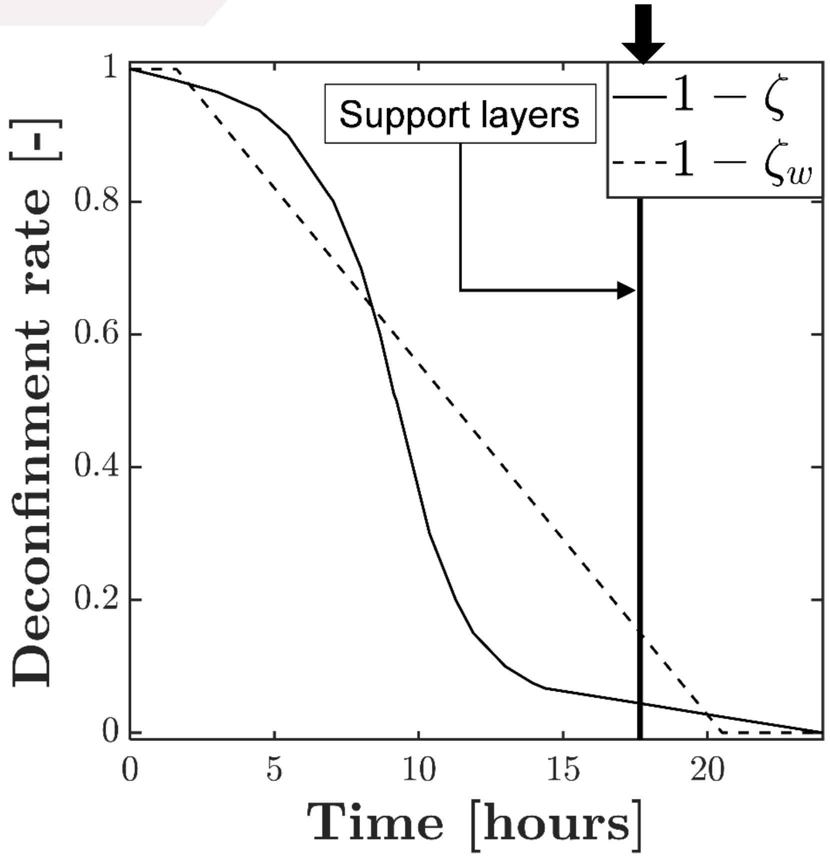

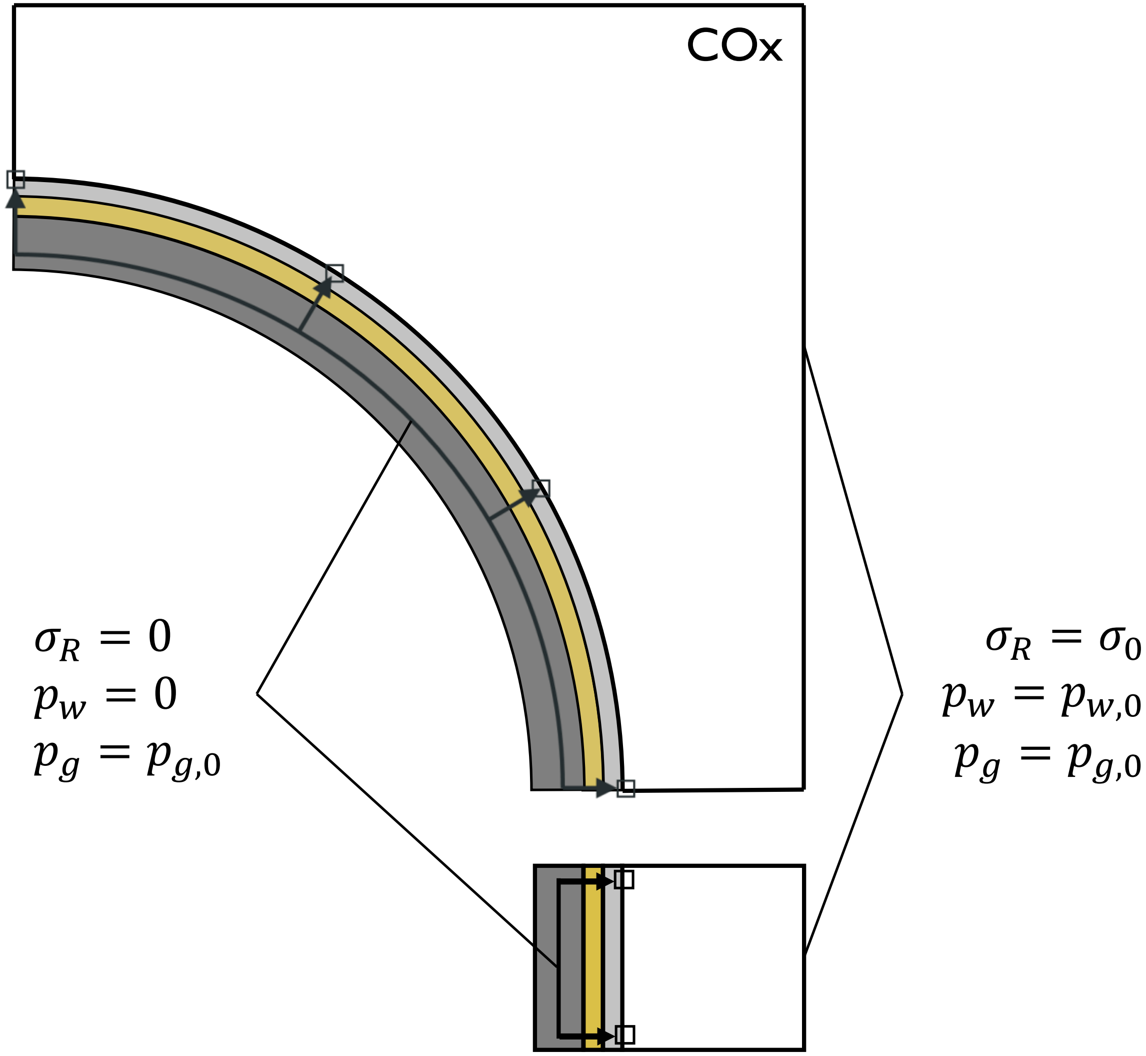

Modelling stages

Step 1 – Ventilation (35 days →100 years)

- Initial step
- Drilling
- Activation of the supports
- Ventilation: conditions regulated at the support wall

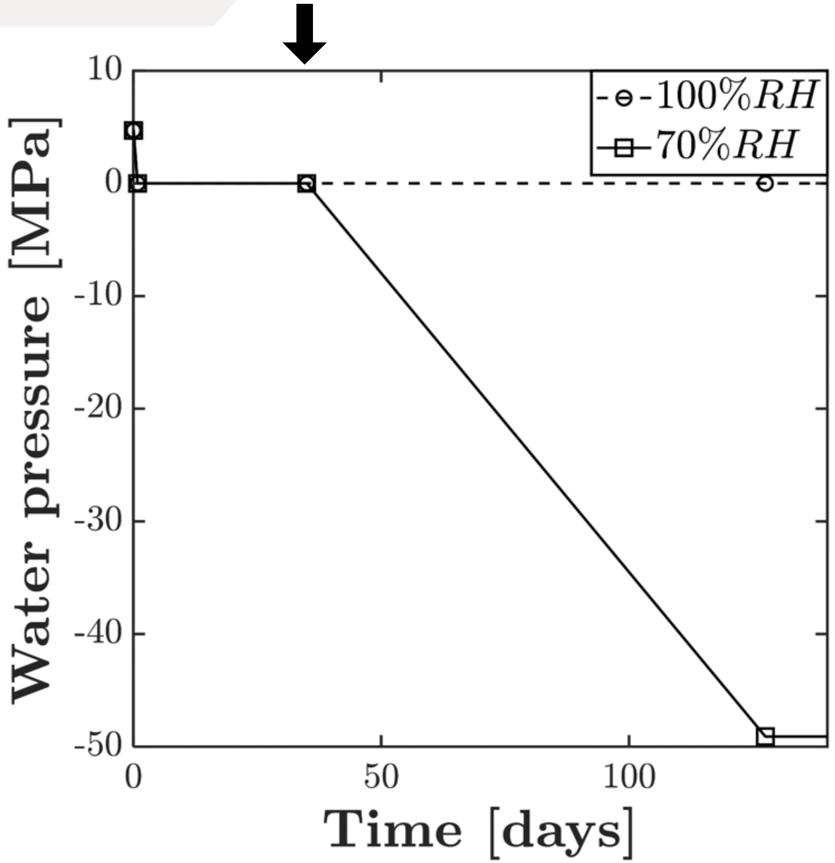

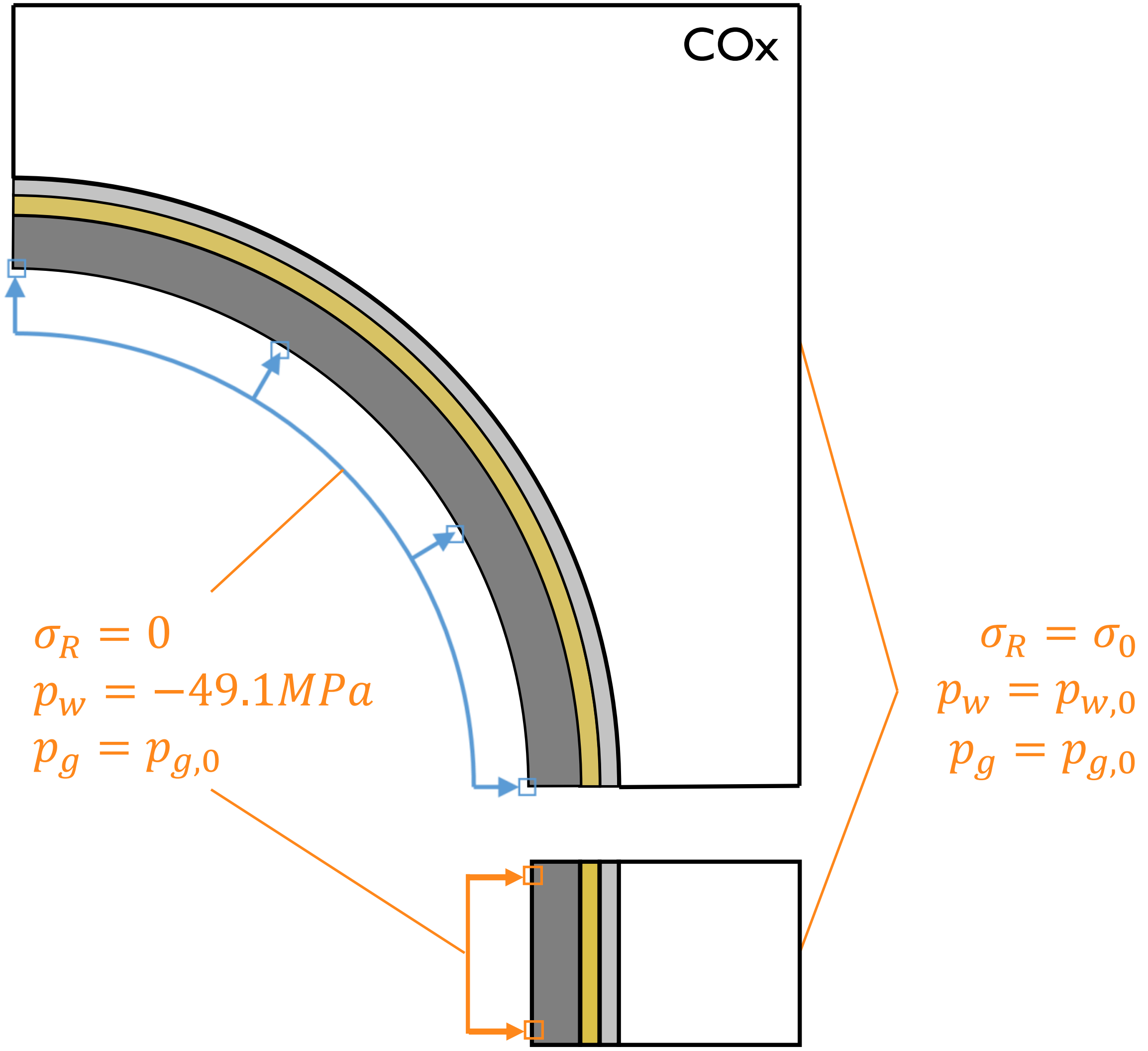

Modelling stages

Step 2 – Pore pressure equilibrium (100 years → …)

- Initial step
- Drilling
- Activation of the supports
- Ventilation
- Gallery in operation:
  - impervious support wall
  - constant gas pressure

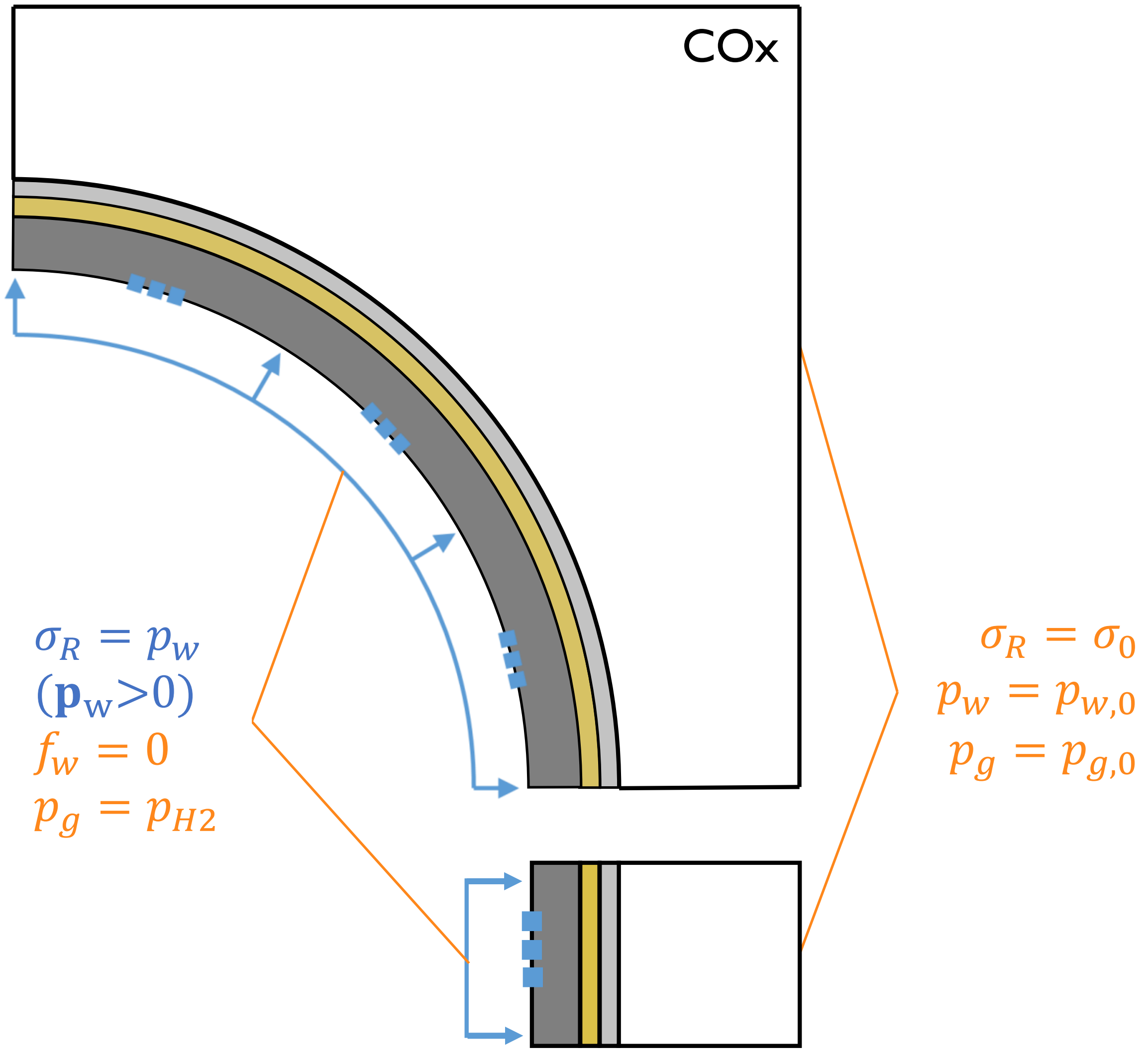

Modelling stages

Step 2 – Gas injection (100 years → 10^6 years)

- Initial step
- Drilling
- Activation of the supports
- Ventilation
- Gallery in operation
- Gas release:
  - impervious support wall
  - imposed H2 pressure at support edge

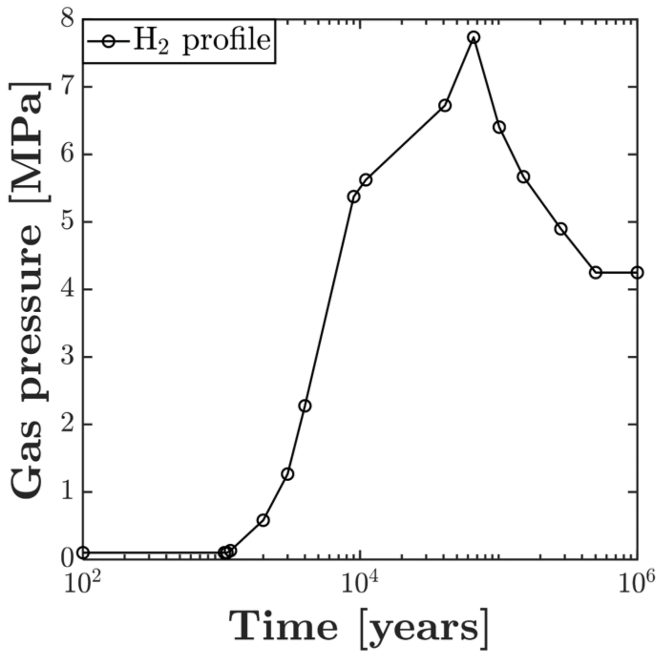

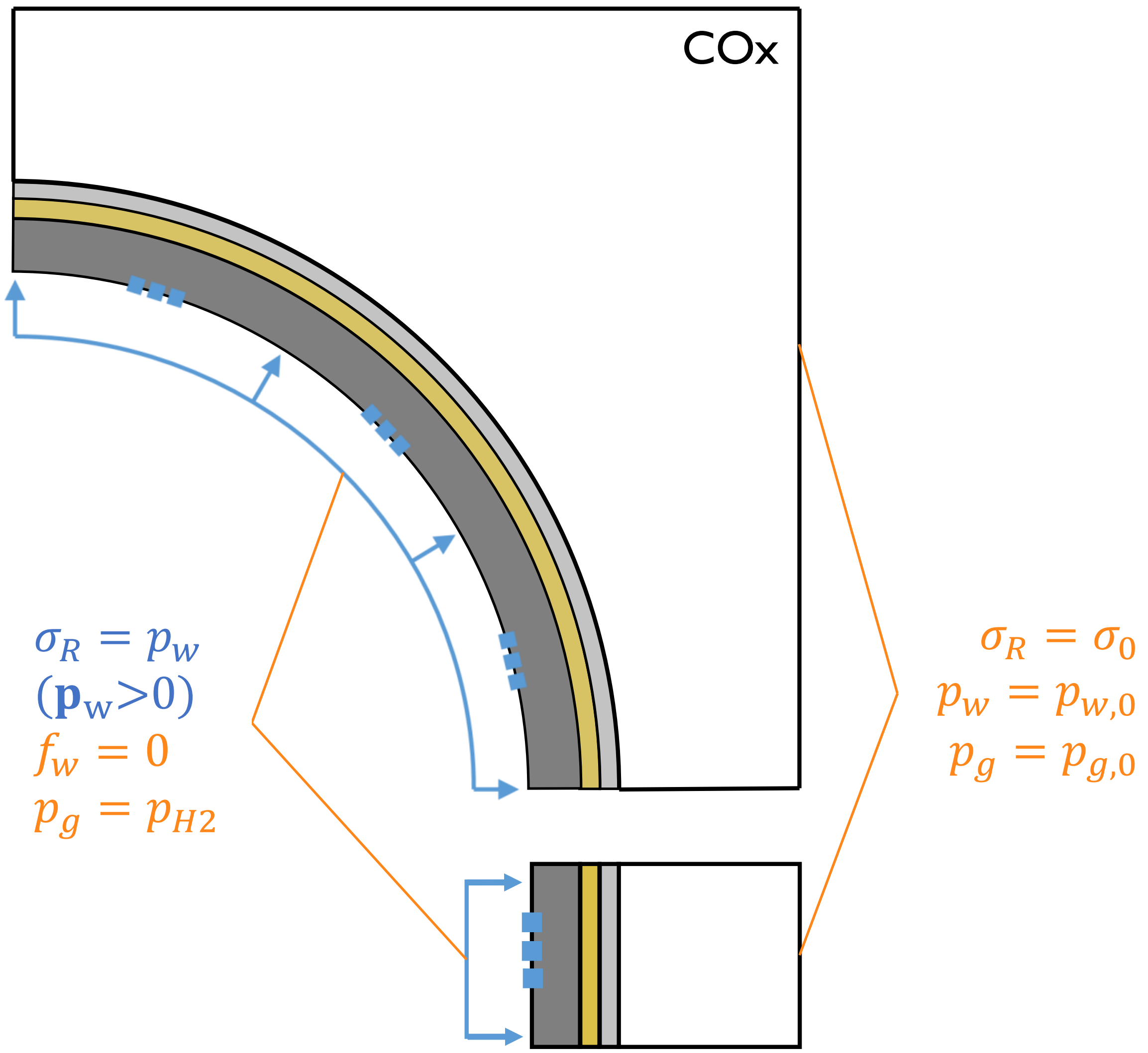

Convergence of the rock mass

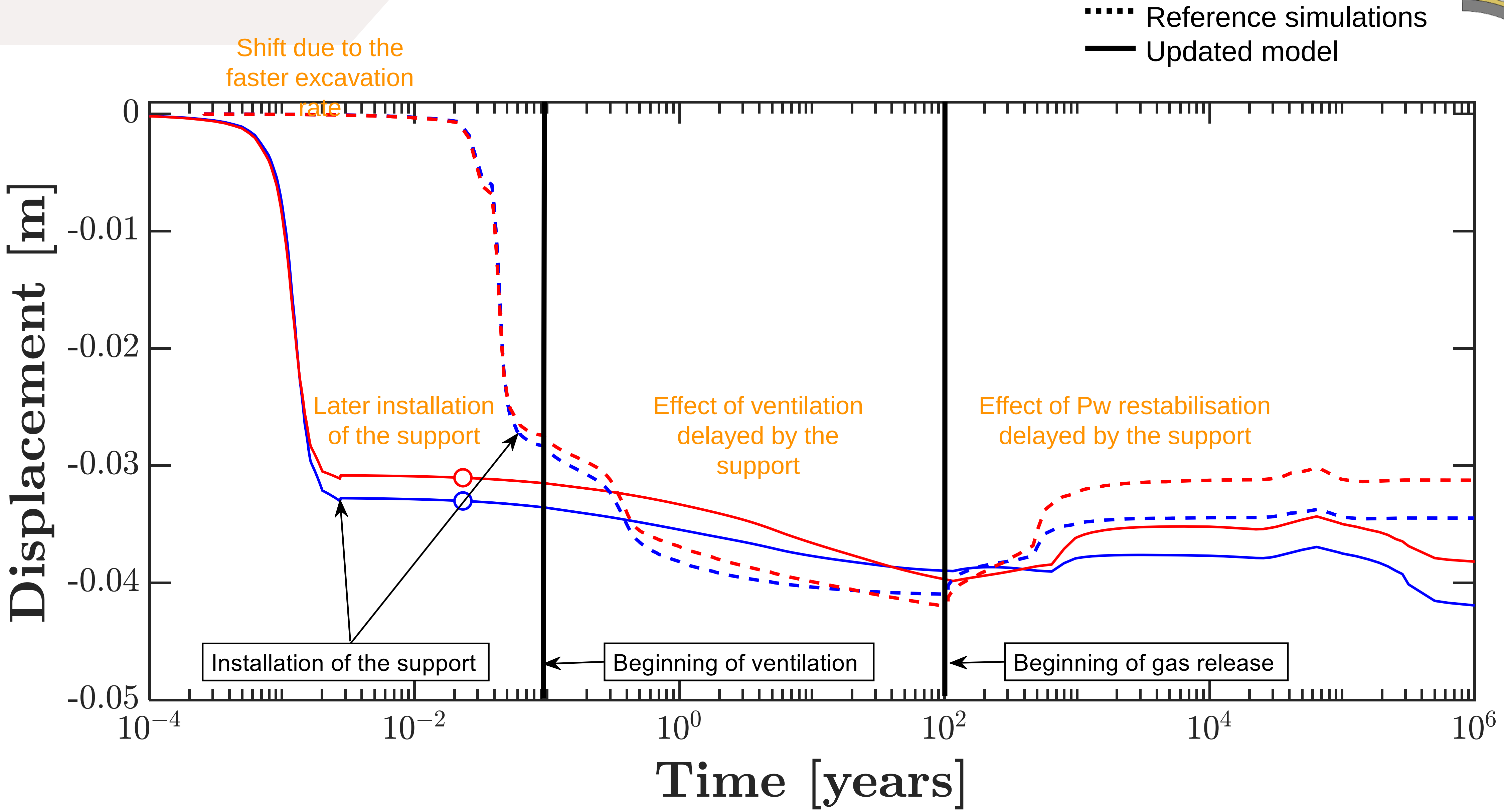

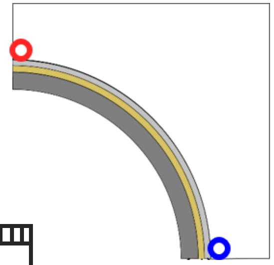

Stresses in the arch segments

LIÈGE université
Urban & Environmental Engineering

Reference simulations
Updated model

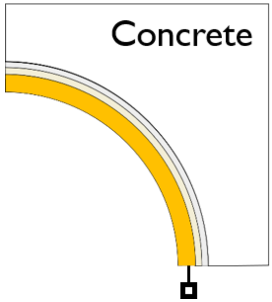

Applied suction induces compression in the concrete

Unloading of the arch segments due to σ_R applied at the intrados

Significant reduction of the effective loading

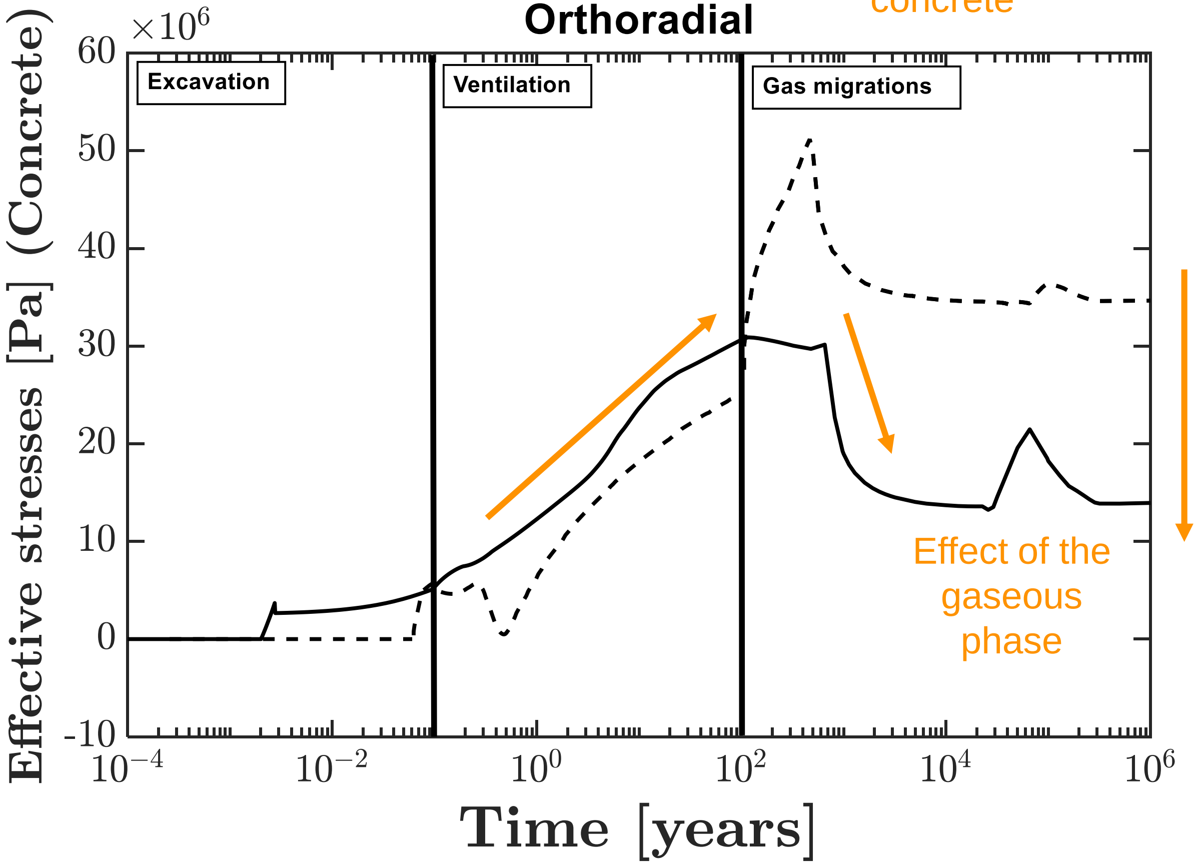

Effect of the gaseous phase

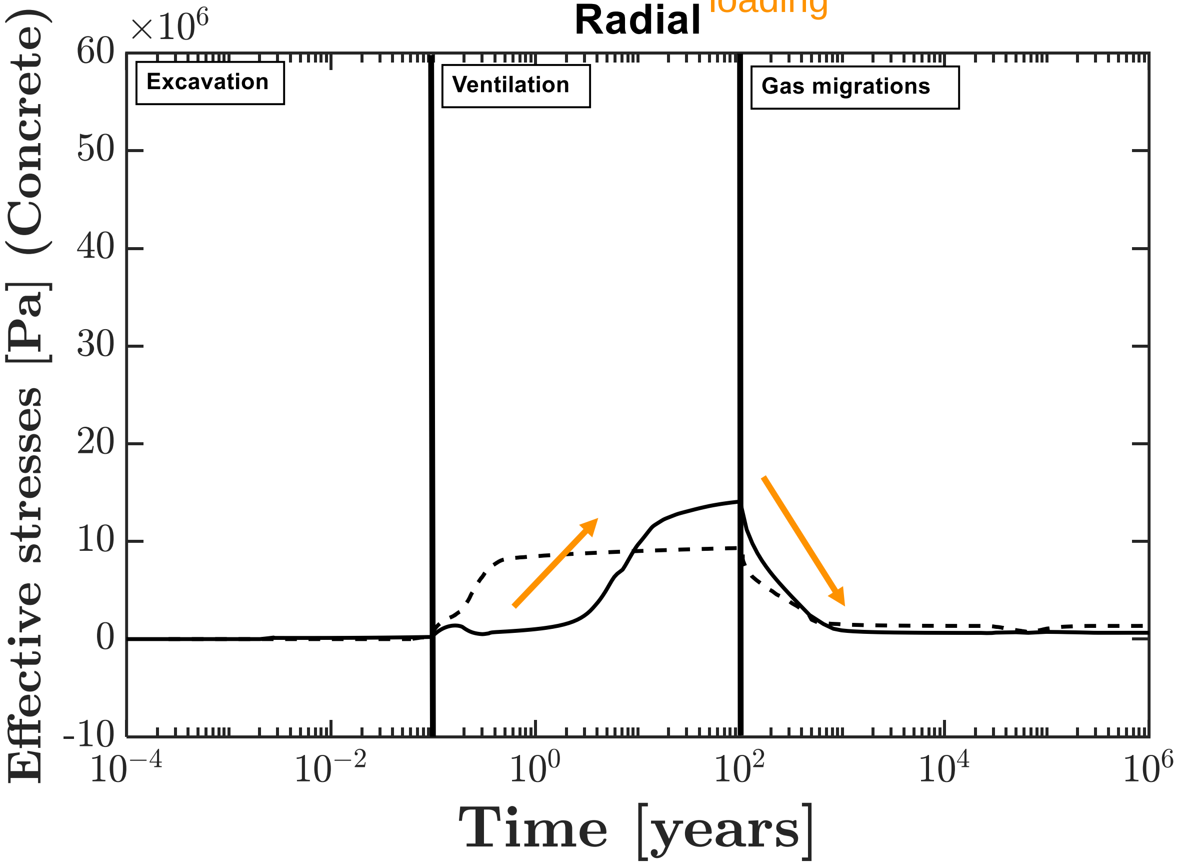

End of the story ?

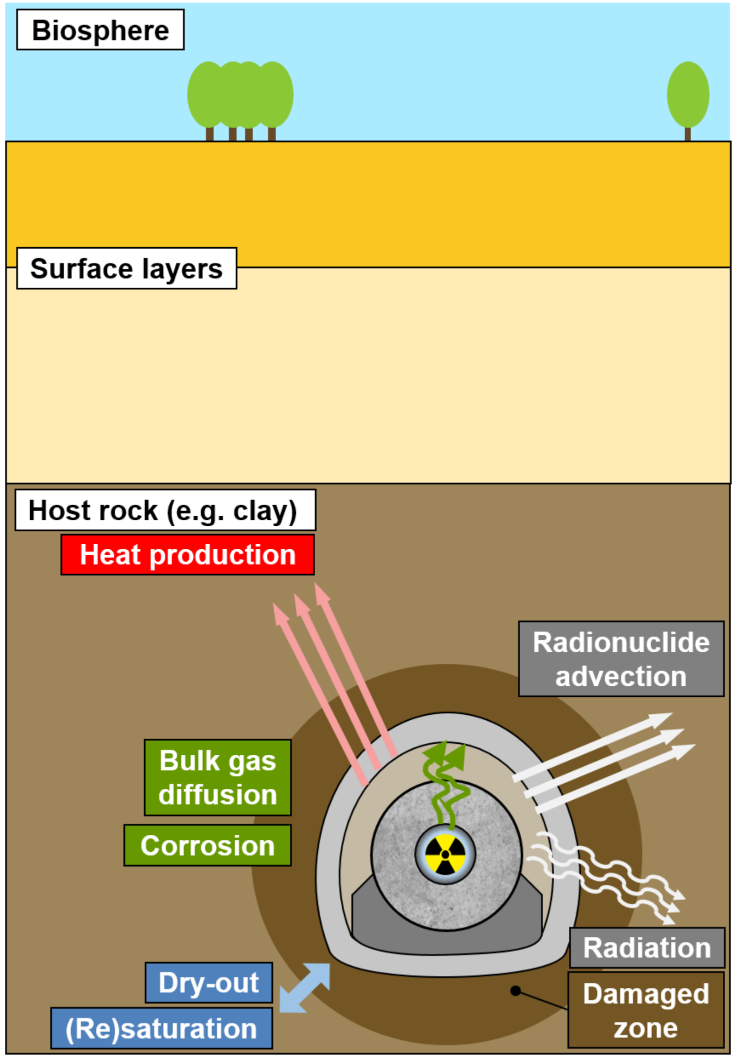

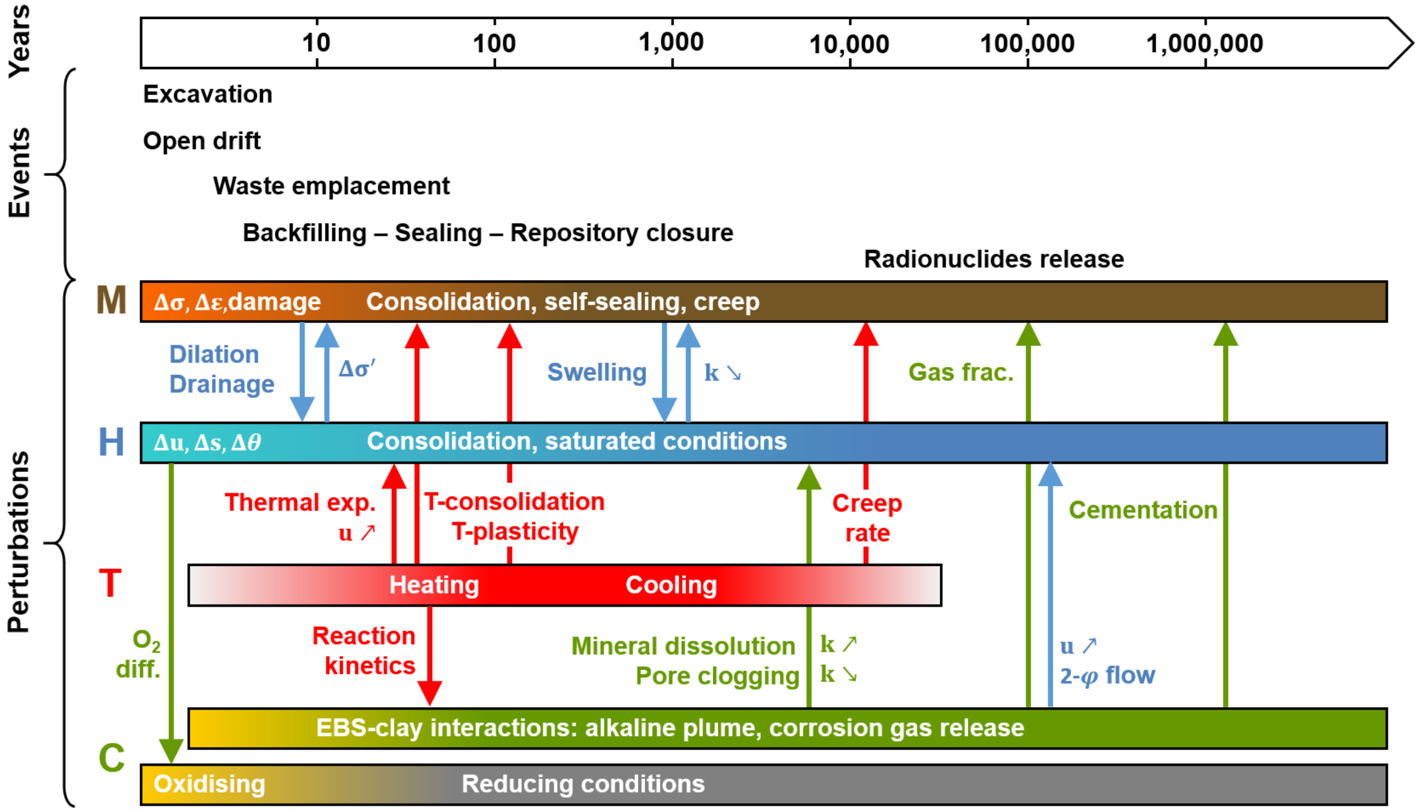

[Sillen, 2012].

Avec le soutien de la

Thank you for your attention.

Numerical Approach

- Classical FE formulation: mesh dependency
- Different regularization methods

Gradient plasticity

Non-local approach

Enrichment of the law

Microstructure continuum

Cosserat model

Second gradient model

Enrichment of the kinematics

Mainly for monophasic materials !

Numerical Approach

In second gradient model, the continuum is enriched with microstructure effects. The kinematics include therefore the classical one but also microkinematics (See Germain 1973, Toupin 1962, Mindlin 1964).

Let us define first the classical kinematics:

- u_i is the (macro) displacement field
- F_{ij} is the macro displacement gradient which means:

$$F_{ij} = \frac{\partial u_i}{\partial x_j}$$

- D_{ij} is the macro strain:

$$D_{ij} = \frac{1}{2}(F_{ij} + F_{ji})$$

- R_{ij} is the macro rotation:

$$R_{ij} = \frac{1}{2}(F_{ij} - F_{ji})$$

Numerical Approach

Enrichment of the kinematics :

The continuum is enriched with microstructure effects: Macro-kinematics + micro-kinematics

Macro Ω:

$$F_{ij} = \frac{\partial u_i}{\partial x_j} = D_{ij} + R_{ij}$$

Micro Ω^m:

$$f_{ij} = \frac{\partial u_i{}^m}{\partial x_j} = d_{ij}{}^m + r_{ij}{}^m$$

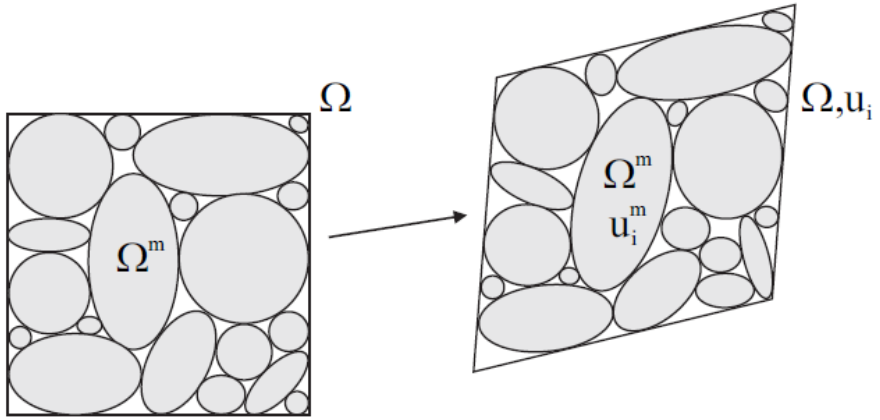

Numerical Approach

In second gradient model, the continuum is enriched with microstructure effects. The kinematics include therefore the classical one but also microkinematics (See Germain 1973, Toupin 1962, Mindlin 1964).

Let us define the micro-kinematics:

- f_{ij} is the microkinematic gradient.
- d_{ij} is the microstrain:

$$d_{ij} = \frac{1}{2}(f_{ij} + f_{ji})$$

- r_{ij} is the microrotation:

$$r_{ij} = \frac{1}{2}(f_{ij} - f_{ji})$$

- h_{ijk} is the (micro) second gradient:

$$h_{ijk} = \frac{\partial f_{ij}}{\partial x_k}$$

Numerical Approach

Second gradient model formulation: weak form

- The internal virtual work (Germain, 1973)

$$W^{*\mathrm{i}} = \int_{\Omega} w^* \, \mathrm{d}v = \int_{\Omega} (\sigma_{ij} D^*_{ij} + \tau_{ij}(f^*_{ij} - F^*_{ij}) + \chi_{ijk} h^*_{ijk}) \, \mathrm{d}v$$

- The external virtual work (simplified)

$$W^{*\mathrm{e}} = \int_{\Omega} G_i u^*_i \, \mathrm{d}v + \int_{\partial\Omega} (t_i u^*_i + T_{ij} f^*_{ij}) \, \mathrm{d}s$$

- The virtual work equations can be extended to large strain problems

Numerical Approach

Second gradient model formulation: strong form

$$\begin{cases} \dfrac{\partial(\sigma_{ij} - \tau_{ij})}{\partial x_j} + G_i = 0 \\ \dfrac{\partial \chi_{ijk}}{\partial x_k} - \tau_{ij} = 0 \end{cases}$$

$$\begin{cases} (\sigma_{ij} - \tau_{ij}) n_j = t_i \\ \chi_{ijk} n_k = T_{ij} \end{cases}$$

Three constitutive equations needed !

Numerical Approach

<u>Local</u> Second gradient model formulation:

- Addition of a kinematical constraint (Chambon et al., 1998; Matsushima et al., 2002)

$$f_{ij} = F_{ij}$$

this implies:

$$f_{ij} = \frac{\partial u_i}{\partial x_j}$$

the virtual work equation reads

$$\int_\Omega \left(\sigma_{ij} D^*_{ij} + \chi_{ijk} \frac{\partial^2 u^*_i}{\partial x_j \partial x_k} \right) \mathrm{d}v = \int_\Omega G_i u^*_i \,\mathrm{d}v + \int_{\partial\Omega} \left(p_i u^*_i + P_i D u^*_i \right) \mathrm{d}s$$

Numerical Approach

Local Second gradient model formulation: strong form

$$\frac{\partial \sigma_{ij}}{\partial x_j} - \frac{\partial^2 \chi_{ijk}}{\partial x_j \partial x_k} + G_i = 0$$

$$\sigma_{ij} n_j - n_k n_j D\chi_{ijk} - \frac{D\chi_{ijk}}{Dx_k} n_j - \frac{D\chi_{ijk}}{Dx_j} n_k + \frac{Dn_l}{Dx_l} \chi_{ijk} n_j n_k - \frac{Dn_j}{Dx_k} \chi_{ijk} = p_i$$

$$\chi_{ijk} n_j n_k = P_i$$

Numerical Approach

LIÈGE université
Urban & Environmental Engineering

<u>Local</u> Second gradient model formulation: weak form

$$\int_{\Omega} \left(\sigma_{ij} \frac{\partial u_i^*}{\partial x_j} + \Sigma_{ijk} \frac{\partial^2 u_i^*}{\partial x_j \partial x_k} \right) d\Omega = W_{ext}^*$$

Local quantities

Introduction of Lagrange multiplier field :

$$\int_{\Omega} \left(\sigma_{ij} \frac{\partial u_i^*}{\partial x_j} + \Sigma_{ijk} \frac{\partial v_{ij}^*}{\partial x_k} \right) d\Omega - \int_{\Omega} \lambda_{ij} \left(\frac{\partial u_i^*}{\partial x_j} - v_{ij}^* \right) d\Omega = W_{ext}^*$$

$$\int_{\Omega} \lambda_{ij}^* \left(\frac{\partial u_i}{\partial x_j} - v_{ij} \right) d\Omega = 0$$

Numerical Approach

<u>Local</u> Second gradient model formulation: weak form

Local Second gradient Finite element

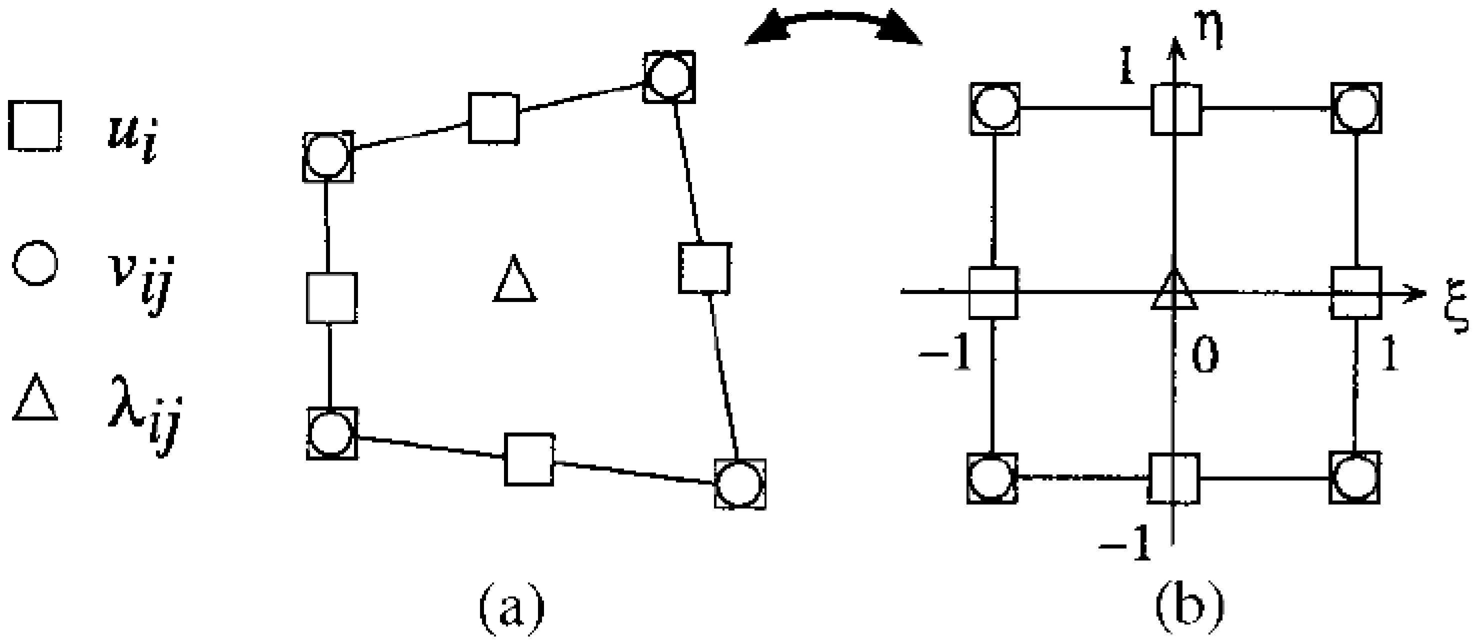

Numerical Approach

Example n°1: Biaxial test (again)

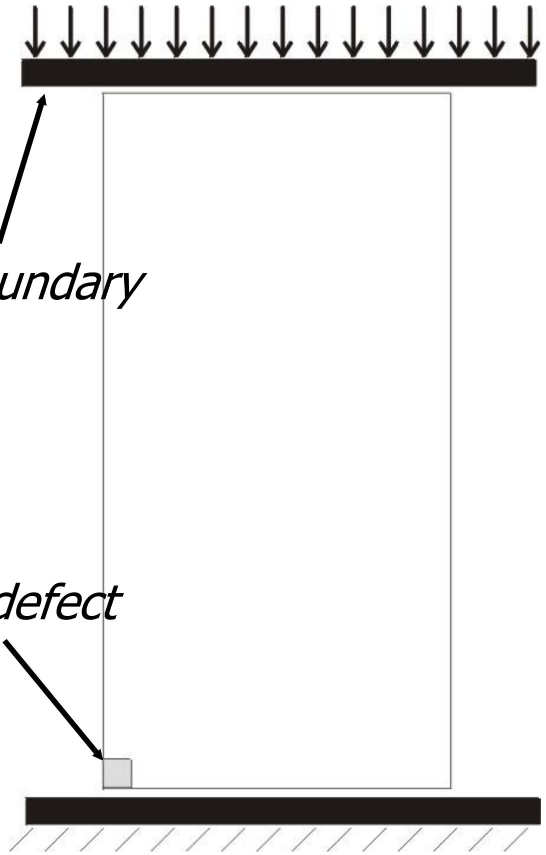

Strain rate : 0.18% / hour

No lateral confinement

Globally drained (upper and lower drainage)

Numerical Approach

Example n°1: Biaxial test (again)

First gradient law

Linear elasticity : E_0 *et* ν_0

Drucker Prager criterion : $$F \equiv \sqrt{\frac{3}{2}} II_{\hat{\sigma}} + m\left(I_{\sigma} - \frac{3c}{\tan\phi} \right) = 0$$

$$m = \frac{2\sin\phi}{3 - \sin\phi} \qquad c = c_0\, f(\gamma^p)$$

Associated softening plasticity (decrease of cohesion) :

$$f(\gamma^p) = \left(1 - (1-\alpha)\frac{\gamma^p}{\gamma_R^p} \right)^2 \; si \; 0 < \gamma^p < \gamma_R^p$$

$$= \alpha^2 \; si \; \gamma^p \geq \gamma_R^p$$

Numerical Approach

Example n°1: Biaxial test (again)

- *Second gradient law :* *Linear relationship deduced from Mindlin*

$$
\begin{bmatrix} \tilde{\Sigma}_{111} \\ \tilde{\Sigma}_{112} \\ \tilde{\Sigma}_{121} \\ \tilde{\Sigma}_{122} \\ \tilde{\Sigma}_{211} \\ \tilde{\Sigma}_{212} \\ \tilde{\Sigma}_{221} \\ \tilde{\Sigma}_{222} \end{bmatrix}
=
\begin{bmatrix}
D & 0 & 0 & 0 & 0 & \frac{D}{2} & \frac{D}{2} & 0 \\
0 & \frac{D}{2} & \frac{D}{2} & 0 & -\frac{D}{2} & 0 & 0 & \frac{D}{2} \\
0 & \frac{D}{2} & \frac{D}{2} & 0 & -\frac{D}{2} & 0 & 0 & \frac{D}{2} \\
0 & 0 & 0 & D & 0 & -\frac{D}{2} & -\frac{D}{2} & 0 \\
0 & -\frac{D}{2} & -\frac{D}{2} & 0 & D & 0 & 0 & 0 \\
\frac{D}{2} & 0 & 0 & -\frac{D}{2} & 0 & \frac{D}{2} & \frac{D}{2} & 0 \\
\frac{D}{2} & 0 & 0 & -\frac{D}{2} & 0 & \frac{D}{2} & \frac{D}{2} & 0 \\
0 & \frac{D}{2} & \frac{D}{2} & 0 & 0 & 0 & 0 & 0
\end{bmatrix}
\begin{bmatrix} \frac{\partial \dot{v}_{11}}{\partial x_1} \\ \frac{\partial \dot{v}_{11}}{\partial x_2} \\ \frac{\partial \dot{v}_{12}}{\partial x_1} \\ \frac{\partial \dot{v}_{12}}{\partial x_2} \\ \frac{\partial \dot{v}_{21}}{\partial x_1} \\ \frac{\partial \dot{v}_{21}}{\partial x_2} \\ \frac{\partial \dot{v}_{22}}{\partial x_1} \\ \frac{\partial \dot{v}_{22}}{\partial x_2} \end{bmatrix}
$$

D = 20 kN

Numerical Approach

Example n°1: Biaxial test (again)

Bifurcation directions (Regularization : Second gradient)

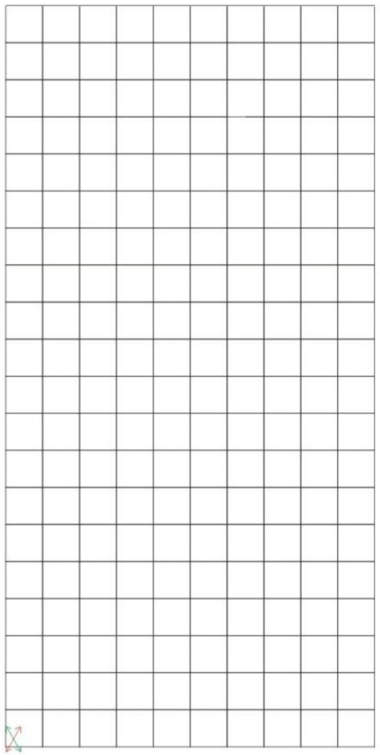

Before

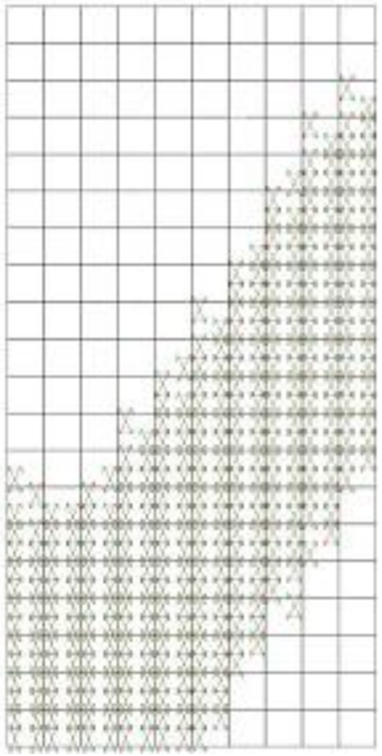

After

Numerical Approach

Example n°1: Biaxial test (again)

Plastic loading point

(Regularization : Second gradient)

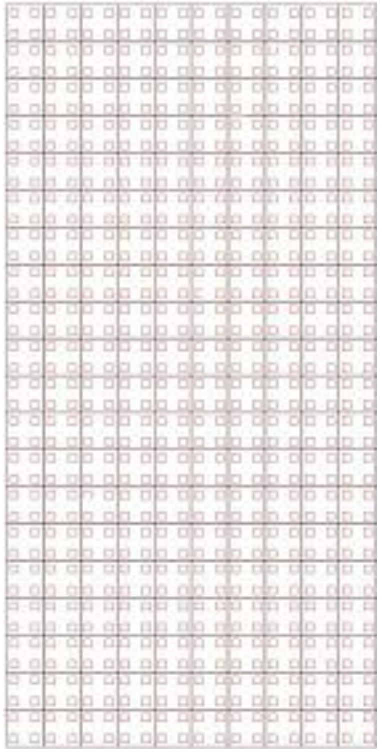

Before

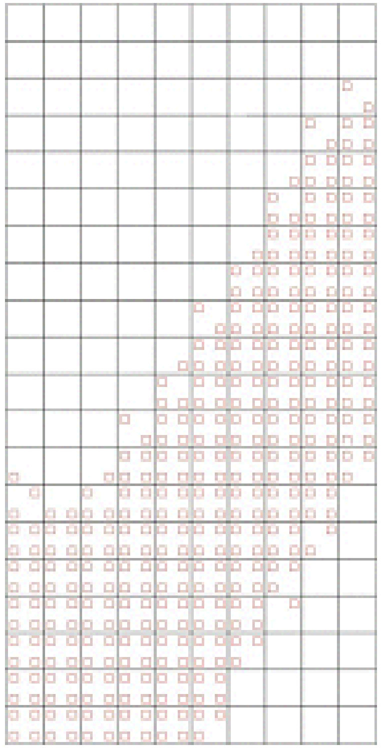

After

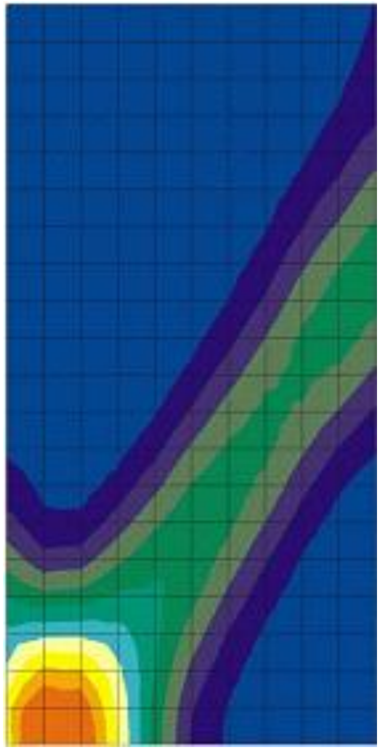

Numerical Approach

Example n°1: Biaxial test (again)

Velocity field

(Regularization : Second gradient)

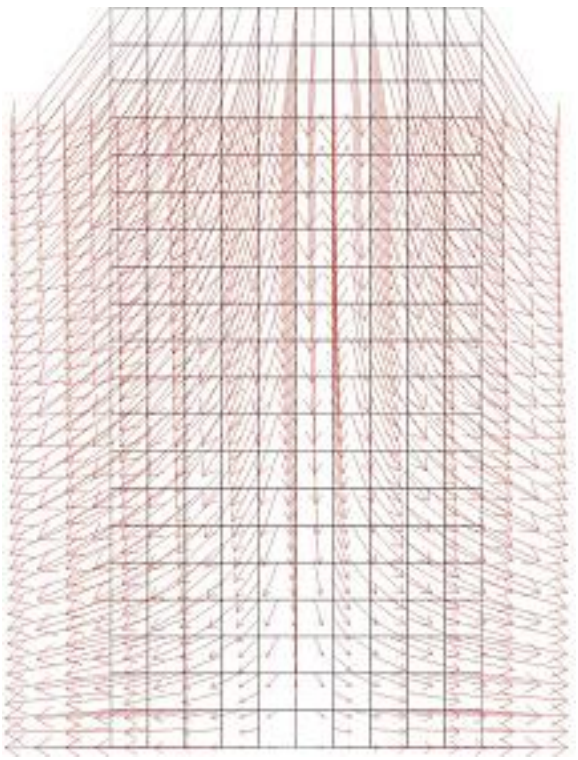

Before

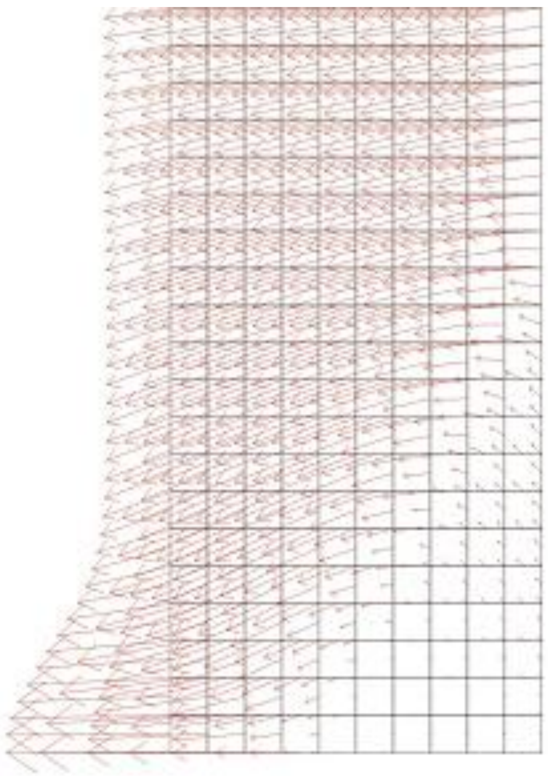

After

Numerical Approach

LIÈGE université
Urban & Environmental Engineering

Example n°1: Biaxial test (again)

Initiation of localization (Directional research – Chambon et al., 2001)

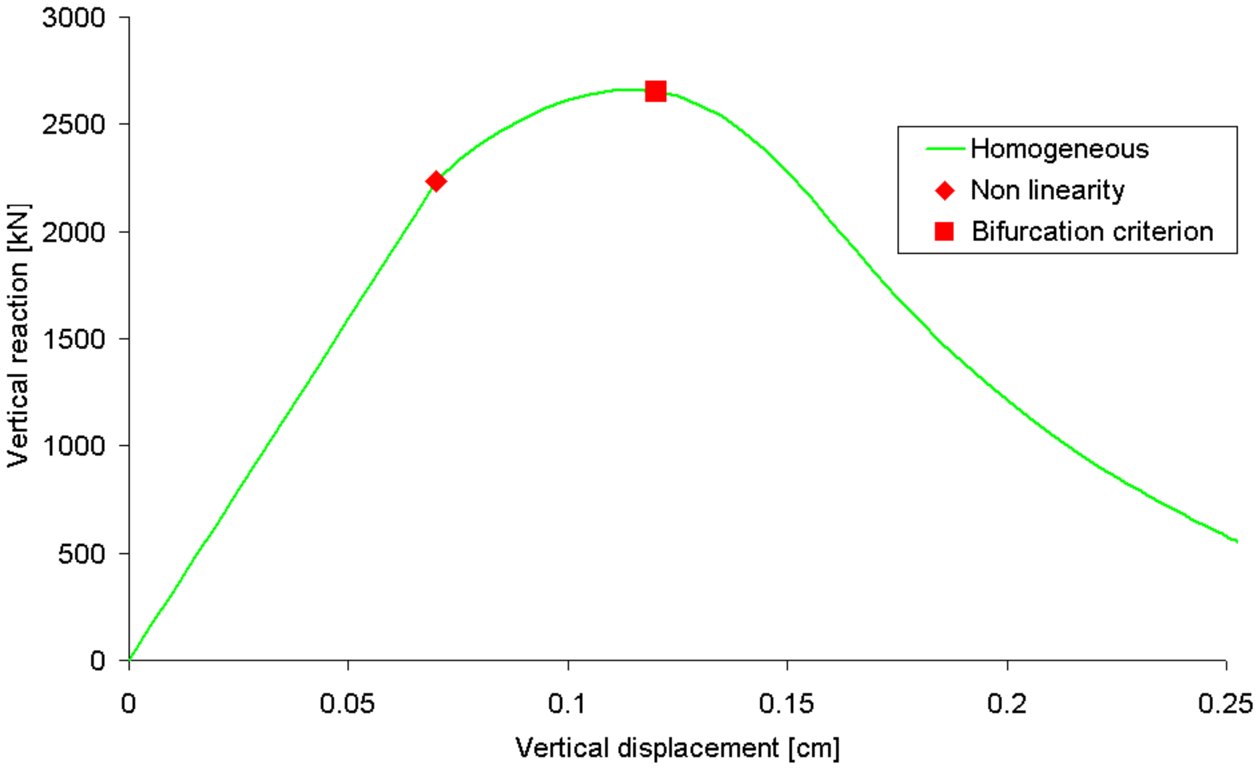

Numerical Approach

Example n°1: Biaxial test (again)

Initiation of localization (Directional research)

(Regularization : Second gradient)

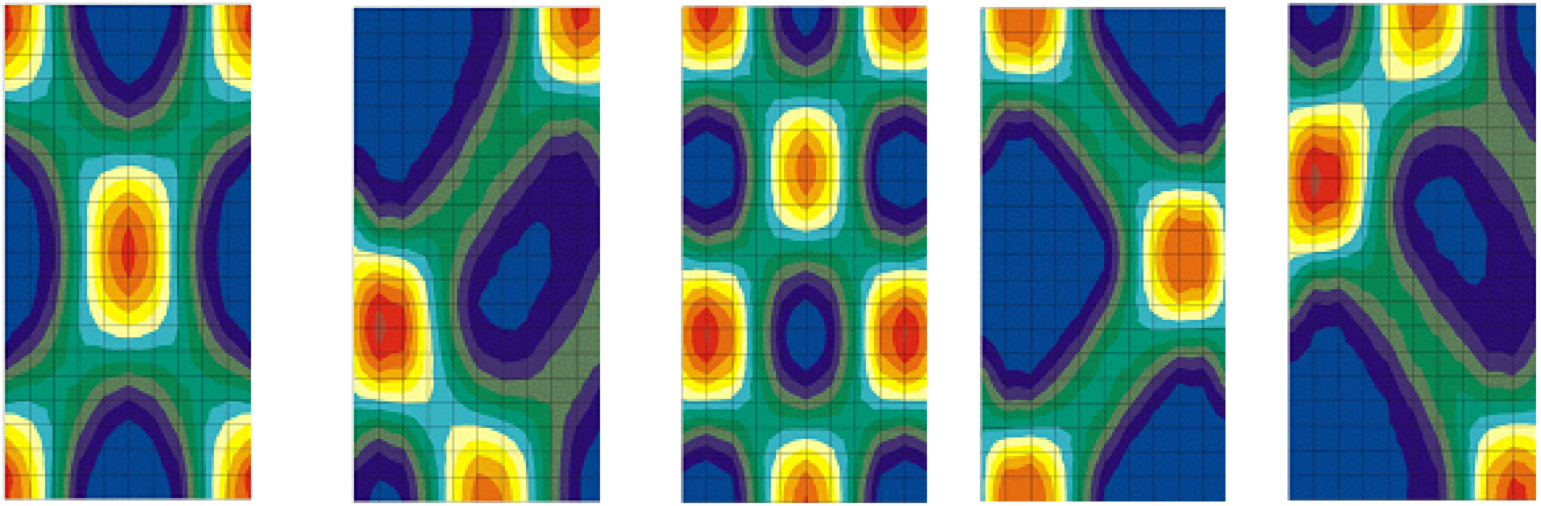

Non uniqueness of the solution

Numerical Approach

Example n°1: Biaxial test (again)

Initiation of localization (Directional research)

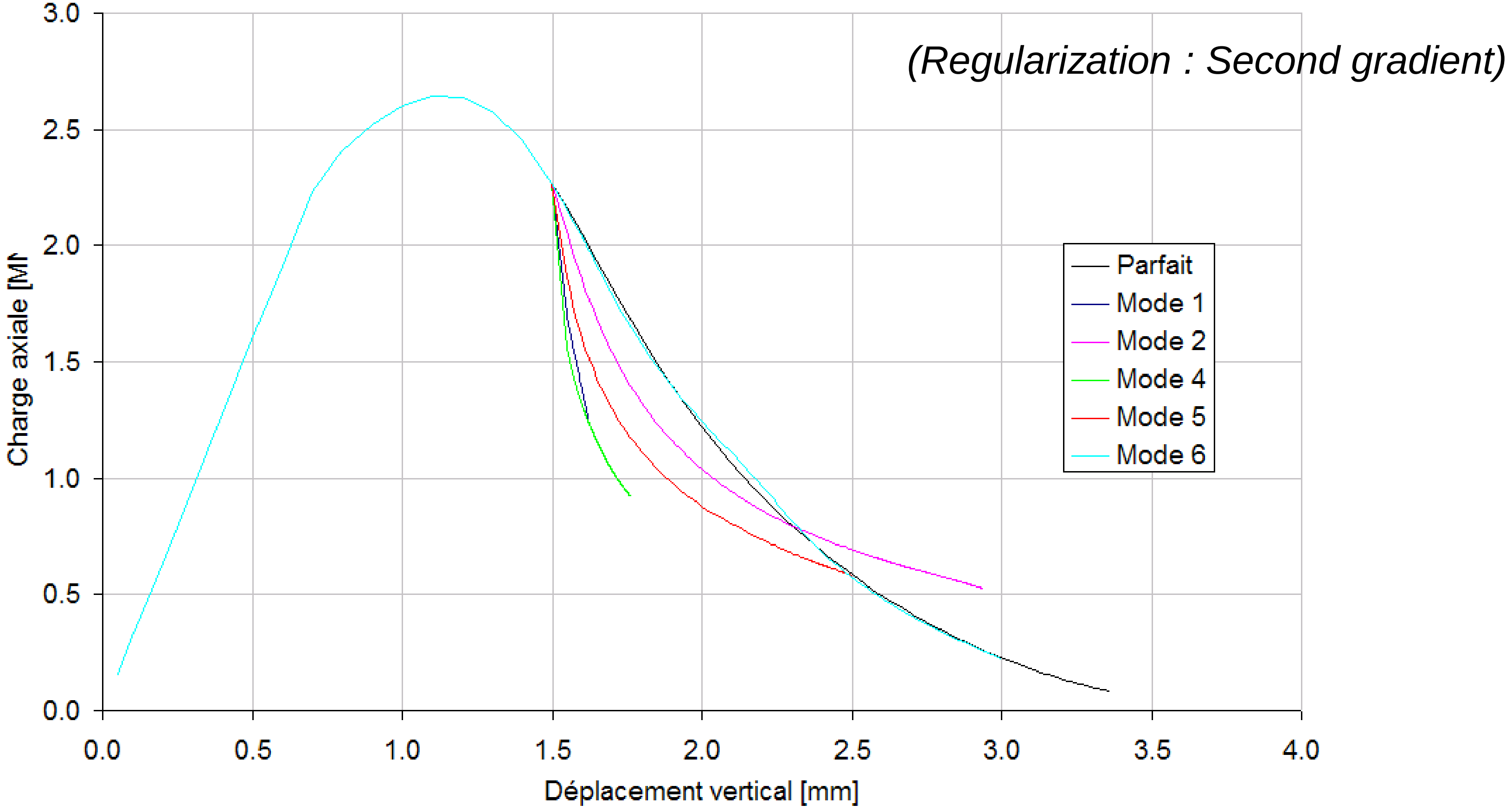

Non uniqueness of the solution

Numerical Approach

Example n°1: Biaxial test (again)

Localization mode switching (Bésuelle et al.,2006)

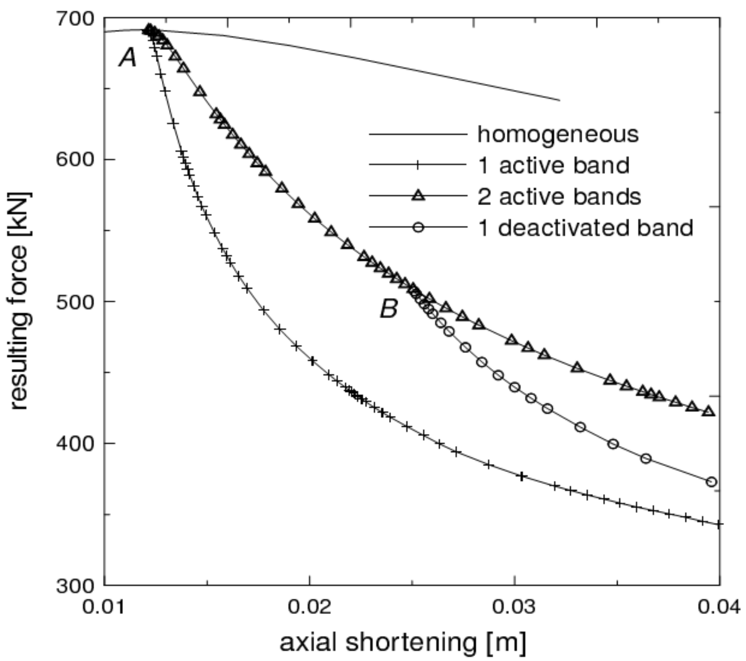

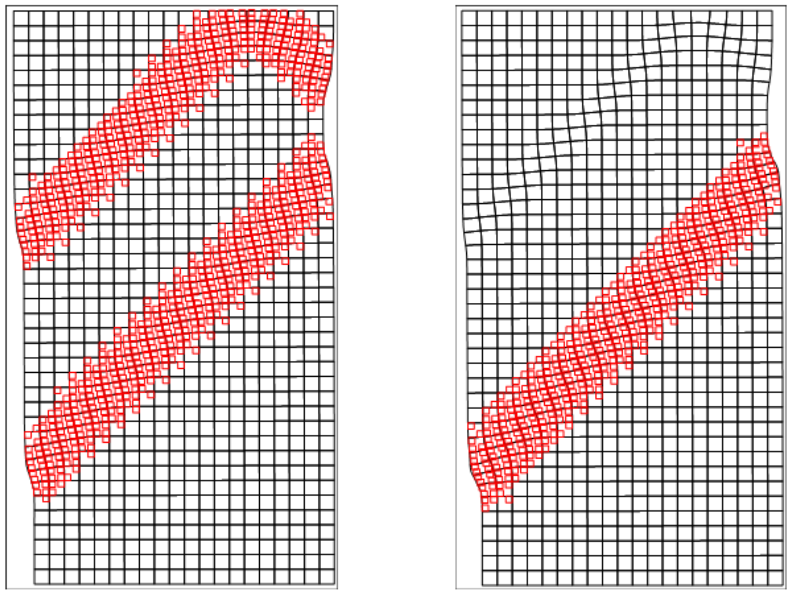

Non uniqueness of the solution

Numerical Approach

Local Second gradient HM model formulation: weak form

- ✓ Second gradient effects are assumed only for solid phase
- ✓ For the mixture, there are stresses which obey the Terzaghi postulate and double stresses which are only the one of the solid phase
- ✓ Boundary conditions for the mixture are enriched

Numerical Approach

Local Second gradient HM model formulation: weak form

$$\int_\Omega \left(\sigma_{ij} \frac{\partial u_i^*}{\partial x_j} + \Sigma_{ijk} \frac{\partial^2 u_i^*}{\partial x_j \partial x_k} \right) d\Omega = W_{ext}^*$$

$$\int_\Omega \dot{M}\, p^* - m_i \frac{\partial p^*}{\partial x_i} d\Omega = \int_\Omega Q\, p^* d\Omega + \int_\Gamma \bar{q}\, p^* d\Gamma$$

Darcy's law $$m_i = -\rho_w \frac{\kappa}{\mu} \left(\frac{\partial p}{\partial x_i} + \rho_w g_i\right)$$

Storage law $$\dot{M} = \rho_w \frac{\dot{p}}{k^w} \phi + \rho_w \frac{\dot{\Omega}}{\Omega}$$

Numerical Approach

<u>Local</u> Second gradient <u>HM</u> model formulation:

Isoparametric Finite Element :

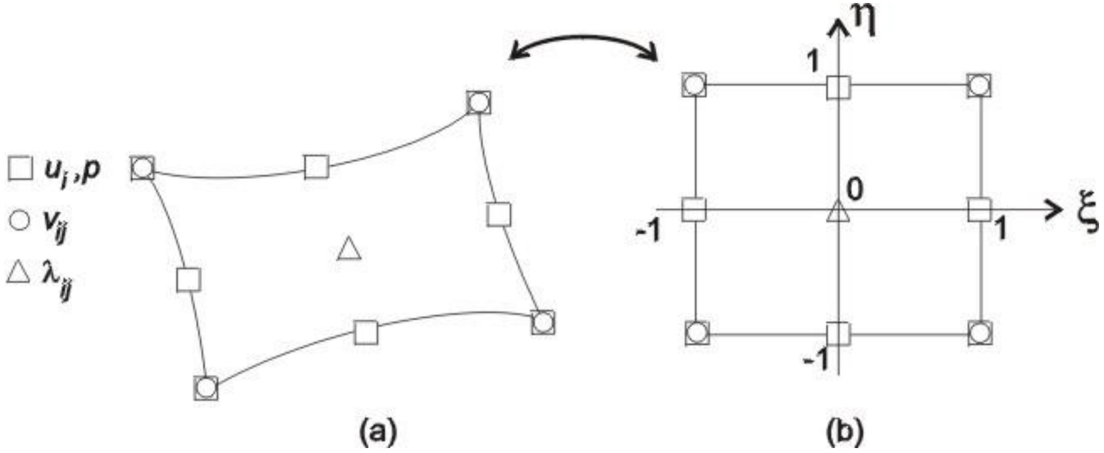

8 nodes for macro-displacement and pressure field
4 nodes for microkinetic gradient field
1 node for Lagrange multipliers field

Numerical Approach

Example n°1: Biaxial test (last time)

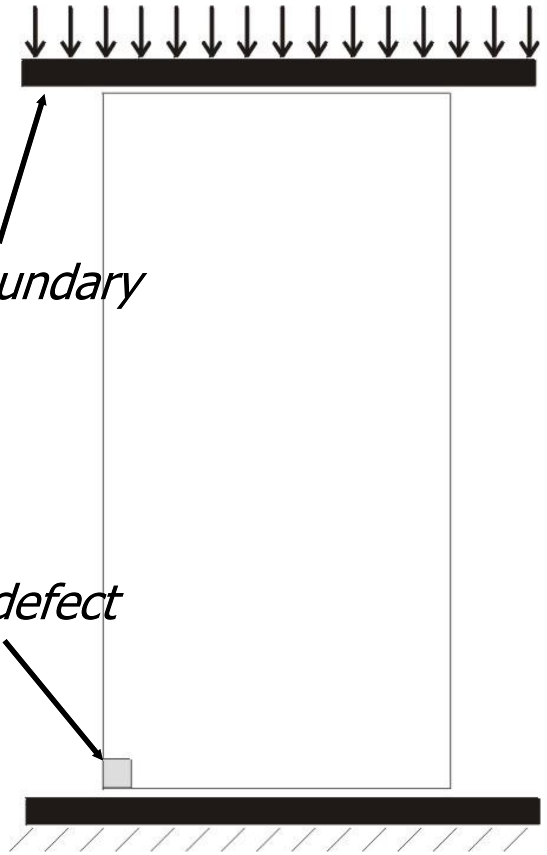

Strain rate : 0.18% / hour

No lateral confinement

Globally drained (upper and lower drainage)

Numerical Approach

LIÈGE université
Urban & Environmental Engineering

- *Equivalent strain after 0.2 % of axial strain ($\kappa = 10^{-12}$ m²)*

(20 x 10) (30 x 15) (40 x 20)

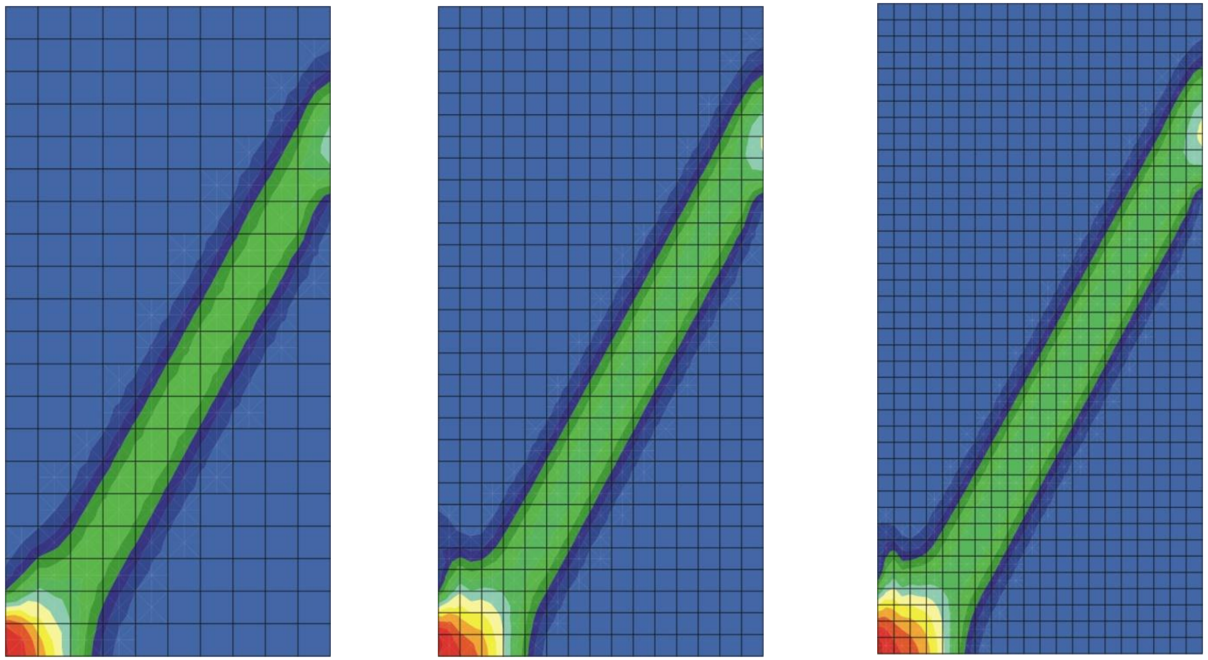

Numerical Approach

- *Plastic loading point after 0.2 % of axial strain ($\kappa = 10^{-12}$ m²)*

(20 x 10) (30 x 15) (40 x 20)

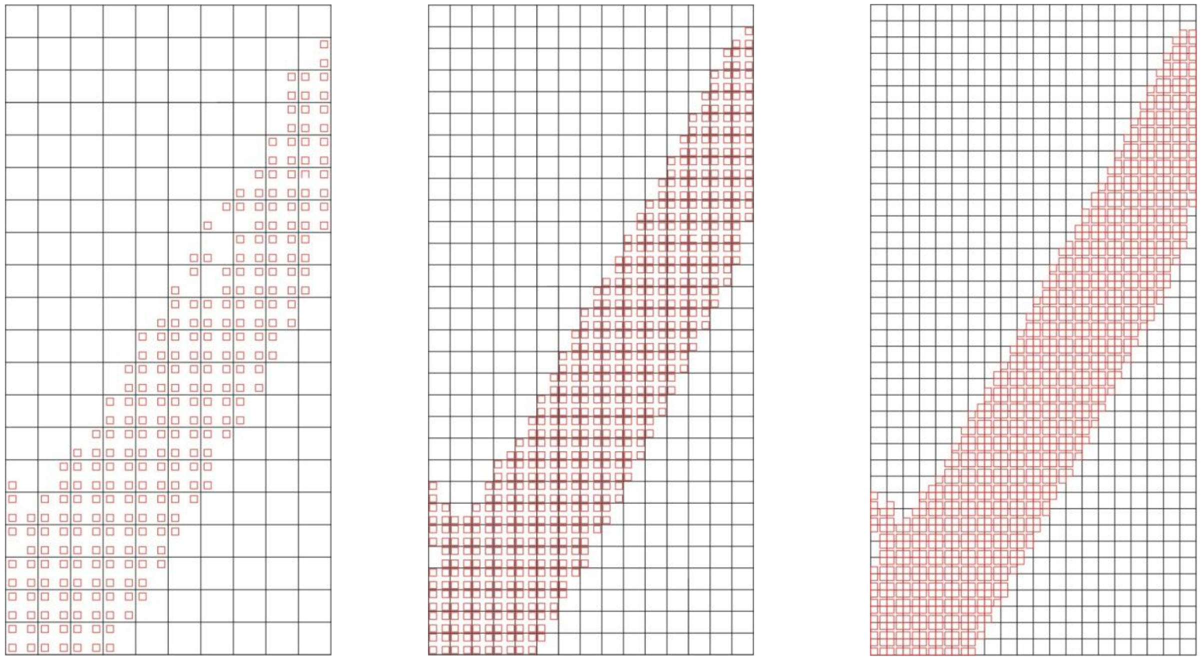

Numerical Approach

Coupled modelling – Comparison Coarse mesh - Refined mesh

Coupled second gradient FE formulation

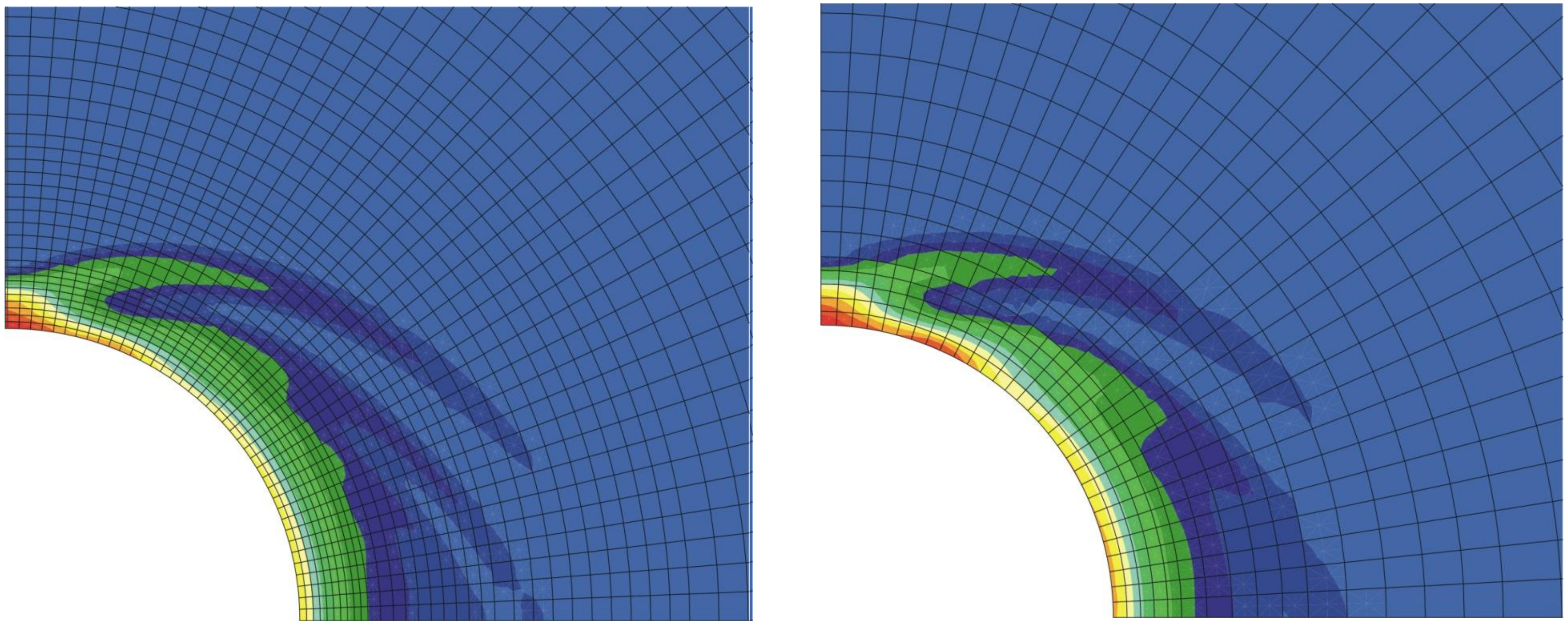

Deviatoric strains

Table of Contents